Viruses in connectomics: Viral transneuronal tracers and genetically modified recombinants as neuroscience research tools

Gabriella Ugolini

Viruses in connectomics: viral transneuronal tracers and genetically modified recombinants as neuroscience research tools

Gabriella Ugolini

PII: S0165-0270(20)30340-X

DOI: https://doi.org/10.1016/j.jneumeth.2020.108917

Reference: NSM 108917

To appear in: *Journal of Neuroscience Methods*

Received Date: 14 April 2020

Revised Date: 12 August 2020

Accepted Date: 14 August 2020

Please cite this article as: Ugolini G, Viruses in connectomics: viral transneuronal tracers and genetically modified recombinants as neuroscience research tools, *Journal of Neuroscience Methods* (2020), doi: https://doi.org/10.1016/j.jneumeth.2020.108917

VSI: Virus technology

Viruses in connectomics: viral transneuronal tracers and genetically modified recombinants as neuroscience research tools.

Gabriella Ugolini

Paris-Saclay Institute of Neuroscience (UMR9197) CNRS - Université Paris-Sud, Université Paris-Saclay, 91198 Gif-sur-Yvette, FR.

***Corresponding author:** Dr Gabriella Ugolini, Paris-Saclay Institute of Neuroscience (UMR9197), Bât 32 CNRS, 1 av de la Terrasse, 91198 Gif sur Yvette, France.

Tel : + 33 1 6982 4158. e-mail: gabriella.ugolini@inaf.cnrs-gif.fr

HIGHLIGHTS

- Reviewing viral-based transneuronal tracing technologies: properties and applications (85)
- Rhabdoviruses and alpha-herpesviruses: cellular receptors, intracellular trafficking (85)
- Differences polysynaptic and monosynaptically restricted viral transneuronal tracers (84)
- Defective chimeric viral recombinants for study and manipulation of neuronal circuits (85)
- Reviewing rabies virus propagation properties explaining human rabies pathophysiology (85)

Abstract

Connectomic studies have become 'viral', as viral pathogens have been turned into irreplaceable neuroscience research tools. Highly sensitive viral transneuronal tracing technologies are available, based on the use of alpha-herpesviruses and a rhabdovirus (rabies virus), which function as self-amplifying markers by replicating in recipient neurons. These viruses highly differ with regard to host range, cellular receptors, peripheral uptake, replication, transport direction and specificity. Their characteristics, that make them useful for different purposes, will be highlighted and contrasted. Only transneuronal tracing with rabies virus is entirely specific. The neuroscientist toolbox currently include wild-type alpha-herpesviruses and rabies virus strains enabling polysynaptic tracing of neuronal networks across multiple synapses, as well as genetically modified viral tracers for dual transneuronal tracing, and complementary viral tools including defective and chimeric recombinants that function as single step or monosynaptically restricted tracers, or serve for monitoring and manipulating neuronal activity and gene expression. Methodological issues that are crucial for appropriate use of these technologies will be summarized. Among wild-type and genetically engineered viral tools, rabies virus and chimeric recombinants based on rabies virus as virus backbone are the most powerful, because of the ability of rabies virus to propagate exclusively among connected neurons unidirectionally (retrogradely), without affecting neuronal function. Understanding in depth viral properties is essential for neuroscientists who intend to exploit alpha-herpesviruses, rhabdoviruses or derived recombinants as research tools. Key knowledge will be summarized regarding their cellular receptors, intracellular trafficking and strategies to contrast host defense that explain their different pathophysiology and properties as research tools.

Keywords: Herpes Simplex, Pseudorabies, Rabies virus, Vesicular stomatitis virus, transneuronal, connectomics.

1. Introduction

The introduction of neuroanatomical tract-tracing method based on anterograde or retrograde axonal transport of markers led to major advances in the understanding of brain functions. Single-step conventional tracers reliably enable the identification of the projections from or to the injection site, and can be combined in multiple tract-tracing paradigms (Morecraft et al., 2014). However, tracing chains of connected neurons is difficult with such methodologies. A major step forward in connectomics has been the development of transneuronal tracers that are transferred specifically between connected neurons and enable the identification of entire functional networks (first-order, second-order, third-order neurons, etc.) (Kuypers and Ugolini, 1990; Ugolini, 2010, 2011). These methodologies initially relied on the use of some conventional tracers, which had low sensitivity and major limitations (Kuypers and Ugolini, 1990; Ugolini, 1995a; Morecraft et al., 2014).

Connectomic studies rapidly became 'viral', as highly sensitive transneuronal tracing techniques were introduced, based on the use of neurotropic viruses as markers, which uniquely function as self-amplifying markers by replicating in recipient neurons (Kuypers and Ugolini, 1990). Within a few decades, viral pathogens were turned into irreplaceable neuroscience research tools (Ugolini, 1995a,b, 1996, 2010, 2011). This review will provide a historical overview of the development of viral-based tracing technologies, and an update of their properties and current applications.

A common characteristic of all transneuronal tracers, including viruses, is that they highjack the cellular internalization and axonal transport machinery. They bind to specific cellular receptors and are internalized through receptor-mediated endocytosis, leading to

efficient uptake even when ligands are present at low concentration. This has two major implications. First, the type and distribution of cellular receptors determines whether a given agent can enter all neuronal cell types (and/or non-neuronal cells), or can lead to uptake restricted to specific cell types. Second, depending on which intracellular transport machinery it highjacks, a given agent can be transported unidirectionally or bidirectionally, and can be exchanged among neurons.

Transfer of substances among neurons can occur via two modalities: a non-specific one (cell-to-cell spread or transcellular transfer), which consists in the exchange among neighboring cells that are not synaptically connected, and a specific one, i.e., transneuronal (transsynaptic) transfer between synaptically connected neurons (Grafstein and Forman, 1980). An effective transneuronal tracer must meet several crucial requirements. First, it should be exchanged exclusively between connected neurons by transneuronal transfer (and not by cell-to-cell spread, which would be a source of error). Second, transneuronal transfer should be unidirectional, to permit unequivocal interpretations. Third, the marker should enable the visualization of all groups of neurons that innervate the injection site directly (first-order neurons) and indirectly (second-order neurons, third-order etc.), to permit a comprehensive mapping. Fourth, the number of synaptic steps should be easily identifiable. Fifth, labeling should be easily detectable, and stable in time. Sixth, the marker should not alter neuronal metabolism for a long time to allow for functional and neurotransmitter studies. Thus, validation of potential transneuronal markers has required a thorough evaluation of the specificity and extent of their transmission in experimental models of known connectivity.

Pioneering efforts in the development of viral transneuronal tracers historically started by trials and errors, because knowledge of intracellular trafficking mechanisms and viral neurotropism was not as advanced as today, and proceeded in parallel. Two main categories of *polysynaptic* viral transneuronal tracers were introduced, based on the use of

wild-type alpha-herpesviruses and rhabdoviruses (Ugolini, 2010). Their specific characteristics will be highlighted and contrasted here. These virus families highly differ in properties that make them useful for different purposes. Only transneuronal tracing with Rabies virus (RABV) is entirely specific and applicable to a variety of species, including primates (Ugolini, 2010). Because these viruses are fully competent for replication, they remain the *only* available tools for polysynaptic tracing of neuronal networks across a potentially unlimited number of synapses. Their use has provided major break-through. Particularly when obtained in primates, results can be immediately translated to the human brain. They are of paramount importance for validating non-invasive imaging techniques and improving the diagnosis and treatment of neurological disorders (Morecraft et al., 2014).

The rapidly expanding viral transneuronal tracing field has fostered extensive cross talk between the neuroscience and virology communities, which has been mutually beneficial. Neuroanatomical studies of virus propagation in well-established models has provided crucial information on the pathophysiology of human rabies (Ugolini, 2008, 2011; Hemachudha et al., 2013; Ugolini and Hemachudha, 2018) and alpha-herpesviruses pathogenesis (Kramer and Enquist, 2013). Implementation of genetic manipulation technologies originally developed by virologists to dissect viral properties have led to recent advances in the development of complementary viral tracers, including a variety of defective and chimeric recombinants derived from alpha-herpesviruses and especially rhabdoviruses, for study and manipulation of neuronal circuits. Their properties and implementations will be described here.

Understanding in depth viral properties is essential for neuroscientists who intend to exploit alpha-herpesviruses, rhabdoviruses or derived recombinants as viral tools in connectomics studies. Thus, this review will provide an update of key knowledge on their cellular receptors, intracellular trafficking and strategies to contrast host cellular defense that explain their different pathophysiology and properties as research tools.

2. Non-viral transneuronal tracers

The first 'transneuronal' tracer was tritium-labeled proline (Wiesel et al., 1974). Because this amino acid is membrane permeable, its anterograde transfer is not truly transneuronal, mostly involving passive diffusion from the transporting fibers to their target area. Among sensitive conventional tracers that are internalized by receptor-mediated endocytosis, transneuronal labelling was obtained exclusively using the lectin Wheat Germ Agglutinin (WGA) and its horseradish peroxidase conjugate (WGA-HRP) and tetanus toxin fragments (TTF) (Kuypers and Ugolini, 1990). Their receptors are N-acetyl-D-glucosamine and sialic acid for WGA (Sawchenko and Gerfen, 1985) and di- and trisialogangliosides for TTF (Bizzini, 1979). A drawback is that WGA-HRP and TTF are transported bidirectionally (Büttner-Ennever et al., 1981; Harrison et al*.,* 1984), which hinders interpretations of the precise routes of labelling. Moreover, transneuronal transfer is very inefficient: it occurs only if first-order neurons are filled with tracer, and only small amounts are transferred. Thus, retrograde transneuronal labeling is very weak and labels only some groups of second-order neurons, depending on the strength and location of their synaptic inputs to first-order neurons (Porter et al., 1985; Horn and Büttner-Ennever, 1990), and on the extent of neuronal activity (Harrison et al., 1984; Jankowska, 1985; Jankowska and Skoog, 1986; Alstermark and Kümmel 1990). Most second-order cell groups are left unlabeled, and third-order neurons cannot be visualized (Porter et al., 1985; Alstermark et al., 1987; Horn and Büttner-Ennever, 1990; Kuypers and Ugolini, 1990; Ugolini, 1995a). For example, we found that transneuronal transfer of WGA-HRP from hypoglossal motoneurons visualized only a small subset of second-order neurons, leaving unlabeled the other premotor cell groups (Ugolini, 1995a). With TTF, transneuronal labeling cannot be confined to the innervation of a single motoneuron pool, because of major spread of TTF from the injected muscle to other muscles (Büttner-Ennever et al., 1981; Horn et al., 1995; Perreault et al., 2006). Moreover, transneuronal labeling disappears with time, and the time

course differs for individual populations, so that they cannot be visualized simultaneously (Horn and Büttner-Ennever, 1990). Because of these major pitfalls, use of non-viral transneuronal tracers was limited to a few studies.

3. How neuroanatomy 'became viral': development of polysynaptic viral transneuronal tracers

In search for more effective transneuronal tracers, the transfer properties of neurotropic viruses started to be examined by neuroanatomists in the eighties (Kuypers and Ugolini, 1990). Highly sensitive transneuronal tracing technologies were developed, based on the use of two classes of viruses with different properties, alpha-herpesviruses and rhabdoviruses (Loewy, 1995; Ugolini, 1995a,b, 1996, 2010, 2011) (Fig. 1).

The first major step forward in the development of viral transneuronal tracers was the introduction of the retrograde transneuronal tracing method based on the use of herpes simplex virus type 1 (HSV 1) (Ugolini et al., 1987, 1989; Kuypers and Ugolini 1990; Ugolini, 1992). Another alpha-herpesvirus with similar properties (Pseudorabies, PrV) was introduced as well (Kuypers and Ugolini 1990; Loewy, 1995; Ugolini, 1995a). These viral tracers, however, had major limitations, as they induce rapid neuronal death and spurious labeling (Kuypers and Ugolini 1990; Loewy, 1995; Ugolini, 1995a) (Figs. 2 and 3).

Continuing the search for a more reliable retrograde transneuronal tracer, I explored the propagation of other viruses, and finally introduced (Ugolini, 1995b) the retrograde transneuronal tracing technology based on the use of a rhabdovirus, rabies virus (RABV) (Ugolini, 2008, 2010, 2011). Among viral transneuronal tracers, only RABV is entirely reliable, because it propagates exclusively by strictly unidirectional (retrograde) transneuronal transfer, while leaving infected neurons viable and intact (Ugolini, 1995b; Ugolini, 2010) (Fig. 4).

The superior sensitivity of viral transneuronal tracing technologies is due to the ability of viruses to function as self-amplifying markers by replicating in recipient neurons, thus

overcoming the 'dilution' problem of conventional tracers and producing intense transneuronal labeling, detected immunohistochemically (Kuypers and Ugolini, 1990; Ugolini, 2010). Because of self-amplification of the tracer signal, viral transneuronal tracing does not require experimental activation of neuronal circuits to enable their comprehensive visualization. When tracing studies are performed using viruses that are fully competent for replication, the viruses behave as *polysynaptic* transneuronal tracers, allowing for the visualization of entire functional neuronal circuits (second-order, third-order neurons etc.), through a potentially unlimited number of synapses.

Regardless of the viral tracer, it is necessary to study the *kinetics* of viral propagation in order to determine the order of connections. Internal controls (known connectivity) must be taken into account to verify the number of synaptic steps crossed at a given time point (Ugolini, 2010). Labeling of first- and higher-order neurons reliably occurs stepwise at different intervals. Each step is determined by the time required for internalization and intracellular axonal transport, plus one cycle of viral replication in recipient neurons. The interval depends upon intrinsic properties of the virus type and strain, as well as the dose administered, and must be determined empirically in any given system (reviewed by Loewy, 1995; Ugolini, 1995a, 1996, 2010; Aston-Jones and Card, 2000). Sensitivity of the immunolabeling detection method is another important factor (Ugolini, 2010).

The virus *dose* is very important: although one virus particle is theoretically sufficient to start the infection, it is necessary to inject a dose above a certain threshold for successful infectivity. Using virus stock at high titer is very important to avoid variability, because infectivity and transneuronal transfer are dose-dependent; high virus concentration guarantees 100% infectivity and serves to maximize transneuronal transfer (Aston-Jones and Card, 2000; Ugolini, 2010). To avoid variability, it is also important to inject virus at the same concentration (possibly from the same batch), administer the same dose in a series of experiments and use the same immunolabeling protocol (Ugolini, 2010).

4. Alpha-herpesviruses

Herpes simplex virus type 1 (HSV 1) is a DNA virus belonging to the alpha-herpesviruses family, which commonly causes cold sores in humans (Ugolini, 1995a, 2010, 2011). By studying its propagation from the hypoglossal nerve and limb nerves in rodents, we demonstrated that HSV 1 could serve to trace neuronal connections transneuronally across at least two synapses (Ugolini et al., 1987, 1989; Kuypers and Ugolini, 1990; Ugolini, 1992, 1995a, 1996, 2010) (Figs. 2 and 3). Transneuronal tracing with HSV 1 was rapidly adapted worldwide for the study of neuronal networks in primates (e.g., Zemanick et al., 1991; Hoover and Strick, 1993). Another alpha-herpesvirus (Pseudorabies, PrV, a swine alpha-herpesvirus) was widely applied for transneuronal tracing studies in rodents (Loewy, 1995; Ugolini, 1995a, 1996, 2010; Aston-Jones and Card, 2000). HSV 1 and PrV have similar properties, but differ in their host range (see Ugolini, 2010).

4.1. Structure, receptors and intracellular cycle

Alpha-herpesviruses are double stranded DNA viruses, with a large linear genome encoding more than 100 genes (Roizman, 1996). The genome is packaged within a capsid, which is overlaid by a tegument and surrounded by a lipid envelope (Fig. 1 A). The viral envelope contains more than twelve glycoproteins, of which at least seven (gB, gC, gD, gH, gL, gE and gI) participate, in different ways, in viral binding, internalization and/or cell-to-cell propagation (Mettenleiter, 2003; Kramer and Enquist, 2013).

Alpha-herpesviruses infect neurons and glial cells, as well as epithelial cells. High-level replication in epithelial cells of the oral and nasal mucosae rapidly evokes immune response. Transneuronal propagation is the net result of the balance between viral neuroinvasiveness, host genetic susceptibility and immune response (Ugolini, 2010). Innate interferon response already acts locally in axons to limit alpha-herpesviruses neuroinvasion (Enquist and Leib,

2016). In its natural host, HSV 1 usually establishes latency in sensory ganglia, with periodic reactivation and centrifugal transport from primary sensory neurons to the innervated site, causing blisters on the lips or oral cavity, or corneal lesions; encephalitis may occur only sporadically, mostly in immunosuppressed individuals or in newborns, where immune response mechanisms are insufficiently developed (Ugolini, 2010; Kramer and Enquist, 2013). With wild-type PrV, virus-related symptoms in pigs and rodents are much more serious (thus its 'Pseudorabies' denomination) (Ugolini, 2010).

The wide cellular tropism of HSV 1 and PrV is due to their recognition of widely distributed cellular receptors. Entry is mediated by primary attachment to heparan sulfate proteoglycans on the cell surface, and interaction with secondary receptors, belonging to the tumor necrosis factor receptor superfamily and the closely related nectin 1 and 2 and poliovirus receptors, members of the immunoglobulin superfamily (Campadelli-Fiume et al., 2000; Mettenleiter, 2003). After receptor binding, the virus particle is internalized by fusion of the viral envelope with the cell membrane; the capsid is released and transported retrogradely to the cell nucleus, where replication involves a temporal cascade of immediate-early, early and late genes (Kramer and Enquist, 2013). Virions mature in the nucleus and gain an envelope by primary budding through the inner nuclear membrane, followed by release of the capsids into the cytoplasm, where the final assembly, including acquisition of the viral envelope, occurs in the trans-Golgi apparatus (Kramer and Enquist, 2013). One cycle of viral replication, that precedes transneuronal transfer, requires 8-16 hrs (Kaplan, 1969; Kristensson et al., 1974).

Because replication of alpha-herpesviruses impairs protein synthesis, it rapidly causes cytopathic changes, typically characterized by a considerable increase in cell size and loss of Nissl staining, which progresses to cell lysis within 2-3 days, and is accompanied *in vivo* by an extensive inflammatory response (Ugolini et al., 1987; Ugolini, 1992; Rinaman et al., 1993; Ugolini, 2010) (Figs. 2 and 3). Uptake and release of HSV 1 and PrV can occur through

dendrites and axons. Axonal transport of HSV 1 and PrV occurs bidirectionally at fast rate (e.g., 8-12 mm/h *in vivo*, Johnson, 1982; 3-5 mm/h in cultured sensory neurons, Lycke et al., 1984; Ugolini, 2010). It is dependent upon recruitment of microtubule-based molecular motor mechanism, involving dynein motors for retrograde axonal transport, and kinesins for anterograde axonal transport (Kramer and Enquist, 2013).

4.2. Host range and age differences

An important difference between HSV1 and PrV is their *host range* (see Ugolini, 2010). Both HSV 1 and PrV are effective transneuronal tracers after CNS and peripheral inoculation in a variety of rodent species (Ugolini, 2010). PrV is also useful in ferrets, but transneuronal tracing studies cannot be performed in primates, because this virus does not infect neurons in monkeys after peripheral or CNS inoculations (Ugolini, 1995a, 2010). In primates, HSV 1 propagates very efficiently by transneuronal transfer after CNS injections (Zemanick et al., 1991; Hoover and Strick, 1993), but not after peripheral inoculations (Ugolini, 1995a, 2010). Another important variable is the *age* of the animals, as susceptibility is age-dependent, being greatest in newborns and lowest in adults, in parallel with progressive maturation of natural defense mechanisms (Ugolini, 2010). Thus, it is preferable to use adult animals of the same age, in order to avoid age-dependent variability in the extent of transneuronal transfer (Ugolini, 1992, 1995a; 2010).

4.3. Peripheral uptake, bidirectional transport and limitations

Major drawbacks of wild-type alpha-herpesviruses are rapid neuronal degeneration (Figs. 2 A,B and 3 E,F) and propagation by spurious (cell-to-cell) spread to glial cells and neurons, which can generate false-positive results (Loewy, 1995; Ugolini, 1995a, 1996, 2010; Ugolini et al., 1987) (Fig. 2 C,D and 3 E). When injected into the CNS, PrV uptake can also involve passing fibers (Chen et al., 1999). PrV can also spread through the cerebrospinal fluid

leading to spurious labeling (Aston-Jones and Card, 2000). Like transneuronal transfer, the extent of local spread of alpha-herpesviruses depends upon the virus strain, dose, and time post-injection (Enquist and Card, 1996; Loewy, 1995; Ugolini, 1995a, 1996; 2010), and can be minimized by manipulating these experimental parameters, but the extent of transneuronal transfer is also reduced (Loewy, 1995; Ugolini, 1995a, 2010). The conditions necessary to minimize local spread (use of attenuated strains containing specific mutations such as Bartha PrV, see # 4.4, injection of low doses and short time points) do not make it possible to trace further than second-order neurons (Loewy, 1995; Ugolini, 1995a, 1996, 2010).

Another major limitation of alpha-herpesviruses is their bidirectional propagation (Ugolini, 1995a, 2010; Aston-Jones and Card, 2000). In rodents, these viruses infect all categories of neurons (sensory, motor and autonomic) that innervate peripheral nerves, muscles, or organs, but propagate more readily in sensory and autonomic pathways, because they have much greater affinity for small sensory neurons and autonomic neurons than motoneurons (Rotto-Percelay et al., 1992; Ugolini, 1992) (Fig. 3). Therefore, they are unsuitable for studying motor innervation, unless sensory and autonomic transfer is prevented by specific lesions (e.g., Fay and Norgren, 1997). Conversely, rabies virus is the ideal tracer for the study of motor pathways, because it enters exclusively in motoneurons (sections # 5.4.1 and 5.9.1).

4.4. Directional selectivity of alpha-herpesviruses due to particular mutations: opportunities

The limitation of bidirectional transfer of alpha-herpesviruses has been overcome by the introduction of the attenuated Bartha strain of PrV, which propagates by retrograde transneuronal transfer (Card et al., 1991, 1992; Loewy, 1995; Ugolini, 1995a; Aston-Jones and Card, 2000). Because of its characteristics, Bartha PrV is particularly suitable for studying autonomic innervation (e.g., Strack and Loewy, 1990; Strack et al., 1999a,b; Standish et al.,

1994; Jansen et al., 1995; Loewy, 1995). The impaired anterograde transfer of Bartha PrV is specifically due to mutations affecting three envelope proteins, gE, gI and Us9, because genetically engineered PrV deletion mutants, lacking the genes encoding these proteins, show the same impairment (Card et al., 1992; Whealy et al., 1993; Standish et al., 1994; Babic et al., 1996; Brideau et al., 2000; Kramer and Enquist, 2013). Notably, these mutations can also affect retrograde transneuronal transfer in some pathways (Standish et al., 1994; Babic et al., 1996), implying that they may not allow a comprehensive retrograde transneuronal mapping of the studied network, unlike wild-type strains (Ugolini, 1995a; 2010). Nonetheless, their unidirectional transfer makes them preferable to wild-type virus. Because of their attenuation, they induce fewer symptoms, and local spread is easier to control.

Directional selectivity was also reported for HSV 1 strains, with strain H129 exhibiting preferential anterograde transport in primates (Zemanick et al. 1991; Kelly and Strick 2003) and rodents (Barnett et al. 1995; Sun et al. 1996; Garner and LaVail 1999). The deficit in retrograde transport of H129 likely involves several genes, because more than 50 % of its genes contain missense or silent mutations (Szpara et al. 2010). Such deficit is incomplete, because temporally delayed retrograde transneuronal transfer can occur (Wojaczynski et al., 2014). In other words, although the transport phenotype of H129 is predominantly anterograde, it also has a retrograde component, that should be taken into account in data analysis. The different directional preference of these particular PRV and HSV 1 strains has been exploited in the construction of recombinants (see # 4.5).

4.5. Alpha-herpesvirus recombinants for dual retrograde or anterograde polysynaptic tracing

An important addition to the transneuronal tracing technology has included the generation of recombinants based on the H129 strain of HSV 1, that either express a reporter marker constitutively (McGovern et al., 2012) or replicate it conditionally upon presence of

Cre recombinase in transgenic mice (Lo and Anderson, 2011). Multiple isogenic H129 recombinants carrying different reporter genes have been generated, that can be visualized simultaneously and enable dual *anterograde* transneuronal tracing (Wojaczynski et al., 2014).

The neuroscientist toolbox also includes a variety of PrV recombinants expressing multiple markers, based on the retrograde transport phenotype of Bartha PrV and gE/gI/Us9 deletion mutants (Enquist and Card, 2003), which enable dual *retrograde* transneuronal tracing studies in rodents (e.g., Billig et al., 2000; Cano et al., 2004). For dual infection of the same cells, it is crucial to avoid that one of the recombinants has competitive advantage, as it would preclude replication of the other recombinant, causing false negative results (Enquist and Card, 2003; Ugolini, 2010). The highest level of successful coinfection is achieved using isogenic recombinants for which the time of infection and transfer within circuits are equivalent. Negative data must be interpreted conservatively, because transneuronal transfer heavily depends upon several factors, including the dose, distance and terminal field density (Card et al., 1999). Thus, it is still possible for one recombinant to reach the cell earlier (e.g., if terminal density is higher in its transporting pathway) and preclude replication of the second virus (Enquist and Card, 2003; Ugolini 2010).

5. Rhabdoviruses

Rabies virus (RABV) belongs to the genus *Lyssavirus* (from the Greek *lyssa*, meaning 'rage') of the rhabdoviruses family. Transneuronal tracing with RABV is entirely specific, enabling polysynaptic tracing across a great number of synapses, as spurious labeling does not occur regardless of the time post-inoculation and infected neurons remain viable and intact (Ugolini, 1995b, 2010) (Fig. 4). Other major advantages of RABV are its strictly unidirectional (retrograde) transport and transneuronal transfer, and its wide host range, that makes it possible to perform studies in primates as well as rodents (Ugolini et al., 2006; Ugolini, 2010). A major ethical advantage is that experimental animals do not exhibit

behavioral changes or any other signs and symptoms of disease during the entire duration of the study, because the time points required for RABV tracing across multiple synapses fall within the long asymptomatic (incubation) period (Ugolini, 2011; Hemachudha et al., 2013).

We have demonstrated that RABV is the specular image of alpha-herpesviruses with regard to peripheral uptake, as it enters exclusively at motor endplates after intramuscular injections in rodents as well as primates (Tang et al., 1999; Graf et al., 2002; Ugolini et al., 2006) (see # 5.9.1). Remarkably, RABV infects only motoneurons and propagates exclusively in motor networks even after injections into mixed nerves (Ugolini, 2008, 2011). Because of its unique properties, it is also the best tool for construction of viral recombinants (see section # 6).

Another rhabdovirus is vesicular stomatitis virus (VSV), from the genus *Vesiculovirus* (from the vesicular lesions that characterize the disease). Importantly, RABV and VSV highly differ in crucial aspects (section # 5.2). For tracing purposes, VSV has major drawbacks because it is highly cytotoxic (section # 5.3), but is useful for construction of chimeric recombinants exploiting its surface glycoprotein, that confers an anterograde transport phenotype (see # 6.3).

5.1. Structure of rhabdoviruses

The rhabdoviruses family (from the Greek *rhabdos*, i.e., 'rod', because of the bullet-shape of the virus particle), to which RABV and VSV belong (Fig. 1 B), includes single strand, negative strand RNA viruses with a small genome (12 kb). They encode only five multifunctional proteins, i.e., a nucleoprotein (N), an RNA-dependent RNA polymerase (L), a polymerase cofactor phosphorylated protein (the phosphoprotein P), a matrix protein (M), and a single external glycoprotein (G) (Dietzschold et al., 2005; Finke and Conzelmann, 2005). The virus particles comprise a central core, containing helical RNA and the N, L and P

proteins, that is associated with the M protein and surrounded by a lipid envelope, on which is anchored the G protein, which protrudes in trimeric spikes (Fig. 1 B) (Schnell et al., 2010).

5.2. Differences between rabies virus (RABV) and vesicular stomatitis virus (VSV)

The properties of RABV and VSV highly differ, because these viruses have evolved in different ways. RABV is a slowly replicating virus (16-20 hrs *in vitro*) with little replication at peripheral sites; it follows a 'hide and seek' strategy, because it needs to escape host antiviral defense and immune response and actively conserve host cell integrity in order to reach the CNS where it amplifies best (Rieder and Conzelmann, 2009; Hemachudha et al., 2013). It has a wide host range in mammals. The infection has a very long incubation, during which the virus propagates extensively within the CNS without inducing symptoms or signs of disease (Ugolini, 2011; Hemachudha et al., 2013). Viremia does not contribute to the RABV cycle.

VSV replicates twice as fast (8-10 hrs *in vitro*) and is a highly cytopathic virus that follows the strategy of 'hit and run', as it does not need to reach the CNS to be transmitted to another host (Rieder and Conzelmann, 2009). It also multiplies in epithelial cells and infects a wide range of mammals and even insects (van den Pol et al., 2009), which can transmit the disease. VSV infection has a very short incubation (3–5 days). It causes major vesicular lesions (resembling foot and mouth disease).

In spite of a similar structure of virus particles, the amino acid sequences of isofunctional VSV and RABV proteins are highly dissimilar (only the N and L display low, segmented homology, Conzelmann et al., 1990). The differences in properties of RABV and VSV are determined especially by their G, M and P proteins. Virus evasion of the intracellular host defense is mainly determined by the P protein for RABV, but the M protein for VSV (Rieder and Conzelmann, 2009; Faul et al., 2009; Oksayan et al., 2012). Differences in the G protein of RABV and VSV determine major differences in host receptors binding and axonal

transport direction, that is exclusively retrograde for RABV, but mainly anterograde for VSV (see # 5.3 and 5.4).

5.3. Vesicular stomatitis virus: intracellular cycle and properties

The broad host and cellular range of VSV is due to its recognition of a highly ubiquitous cellular receptor (the low density lipoprotein receptor, which regulates cholesterol homeostasis) (Finkelshtein et al., 2013). Following G-mediated binding, VSV is internalized by clathrin-mediated endocytosis (Belot et al., 2019). Infection is characterized by rapid general shutdown of host gene expression and severe cytopathic effects, due to multiple activities of the M protein affecting host polymerase functions, mRNA nuclear export and cellular interferon (IFN) response, and high-level virus replication (Rieder and Conzelmann, 2009; Oksayan et al., 2012).

Unlike RABV, VSV propagates bidirectionally *in vivo*, with a first phase involving anterograde transneuronal transfer, and also infects non-neuronal cells; in rodents, the infection is rapidly lethal and severe cell loss occurs very rapidly (Lundh et al., 1987, 1988; Kuypers and Ugolini, 1990). The possibility of non-specific labeling is another major pitfall. Propagation of wild-type VSV was studied in rodents after intranasal instillation (Lundh et al., 1987, 1988; Huneycutt et al., 1994; Plakhov et al., 1995; Cornish et al., 2001), intradermal inoculation (Cornish et al., 2001) or injection into the vitreous body (Lundh, 1990). After intranasal instillation, VSV infects with much greater efficiency the olfactory epithelium than the respiratory epithelium; it propagates in olfactory pathways first anterogradely to the olfactory bulb, and then bidirectionally to higher-order structures (Lundh et al., 1987; Huneycutt et al., 1994; Plakhov et al., 1995; Cornish et al., 2001). Viremia and infection of ependymal cells and cerebrospinal fluid also occur, leading to non-specific infection of neuronal structures abutting the ventricular surface (Huneycutt et al., 1994; Plakhov et al., 1995; Cornish et al., 2001). Bidirectional transfer of VSV was also reported following

unilateral injection into the vitreous body, with rapid anterograde propagation from retinal ganglion cells to the lateral geniculate nucleus and superior colliculus at 12-36 hrs, and retrograde transneuronal labeling of retinal ganglion cells of the non-injected eye one day later (Lundh, 1990). Wild-type or recombinant VSV can also infect primary sensory neurons, although not as prominently as alpha-herpesviruses (Lundh et al., 1987; Plakhov et al., 1995; Beier et al., 2013); intradermal inoculations lead to extensive propagation to the spinal dorsal and ventral horn and bidirectional transfer to supraspinal structures (Cornish et al., 2001).

Anterograde axonal transport of VSV is determined by its G protein (Beier et al., 2013; Haberl et al., 2015) and occurs at high speed (estimated 6-30 mm/day *in vivo)* (Lundh, 1990). The mechanisms involved in bidirectional transfer of VSV that occurs at higher stages of propagation remain unclear. In conclusion, VSV is not very valuable as transneuronal tracer. Its major drawbacks (rapid cell loss, spurious labeling, bidirectional transfer), are paradoxically similar to herpesviruses, although they are mediated by dissimilar viral mechanisms. Due to its pantropic infectivity and high cytotoxicity, VSV is a promising tool for oncolytic protocols designed to target and destroy tumor cells by VSV-induced oncolysis (Melzer et al., 2017), and for developing VSV-based vaccination protocols against tumor antigens (Kottle et al., 2011) and viruses (Schell et al., 2011). For tracing purposes, however, a major limitation of VSV is its rapid cytotoxicity, that is reduced but not abolished in attenuated VSV recombinants containing gene mutations of the M protein (M51) or N protein (N_{R7A}) (van den Pol et al., 2009; Beier et al., 2011; Beier, 2019; Lin et al., 2020) (section # 6.3).

5.4. Rabies virus: intracellular cycle and properties

The surface glycoprotein G of RABV has multiple roles in the viral intracellular cycle. The G protein has an external domain, a transmembrane domain and a cytoplasmic domain.

Its *external* domain is crucial for binding to neuronal receptors and receptor-mediated internalization (Dietzschold et al., 1985; Faber et al., 2004; see section # 5.4.1). It is also the major RABV antigen responsible for induction of protective antibodies (Coulon et al., 1983; Dietzschold et al., 1983, 1985; Huang et al., 2017). Point mutation at position 333 within a major antigenic site of the G external domain (Coulon et al., 1983; Dietzschold et al., 1983) drastically reduces rabies virus neuroinvasiveness (Dietzschold et al., 1985; Coulon et al., 1989; Lafay et al., 1991). The G protein determines the kinetics of virus internalization (Dietzschold et al., 1985; Faber et al., 2004) and is crucial to confer retrograde axonal transport properties to RABV and derived recombinants (Dietzschold et al., 2008). Deletion of the G gene from the RABV genome (Mebatsion et al., 1996a) abolishes transneuronal propagation (Etessami et al. 2000), and genetic replacement or transcomplementation restores neuroinvasiness (Dietzschold et al., 2005, 2008; Finke and Conzelmann, 2005). The G protein also plays an important part in budding, together with the M (Mebatsion et al., 1996a, 1999; Schnell et al., 2010). The G *cytoplasmic* domain determines the level of expression of the G itself (Huang et al., 2017) and of other viral proteins (Bertoune et al., 2017), and is required for the incorporation of foreign glycoproteins into the virion (Schnell et al., 2010). It also manipulates neuronal homeostasis and actively promotes neuronal survival, by specifically targeting the PDZ domain of neuronal enzymes to abrogate virus-mediated apoptosis (Prehaud et al., 2010; Caillet-Saguy et al., 2015).

5.4.1. Rabies virus Receptors

Internalization of RABV is mediated by interaction of the G with cellular receptors. RABV propagates in a wide variety of neuronal types in the CNS, suggesting a ubiquitous distribution of its cellular receptors (Ugolini, 2010) (see # 5.7). Among the molecules that have been proposed to act as cellular receptors for RABV, the neuronal cell adhesion molecule (NCAM) (Thoulouze et al., 1998) is the most likely candidate (Lafon, 2005), in view

of its widespread distribution (Ugolini, 2010). NCAM clearly acts as a major RABV receptor *in vivo,* because in NCAM-deficient mice RABV neuroinvasion is drastically restricted, although not entirely abolished, suggesting that additional receptors may be also utilized (Thoulouze et al., 1998). Another putative RABV receptor, the p75 neurotrophin receptor (p75NTR, low affinity nerve growth factor receptor) (Tuffereau et al., 1998) is not sufficiently ubiquitous (Ugolini, 2010), and is not essential for RABV infection, as the time course and extent of RABV neuroinvasion are indistinguishable in p75NTR-deficient and wild-type mice (Jackson and Park, 1999; Tuffereau et al., 2007). Moreover, specific dorsal root ganglia (DRG) populations that express p75NTR are not infected (Tuffereau et al., 2007).

Another RABV receptor, the nicotinic acetylcholine receptor (nAChR) (Lentz et al., 1982; Hanham et al., 1993), is very important for peripheral uptake. Because of its postsynaptic location at motor endplates, it determines RABV entry in muscle cells, and concentrates viral particles at the neuromuscular junction, facilitating NCAM-mediated internalization at the presynaptic site (Lafon, 2005; Ugolini, 2010). Presence of the nAChR at motor endplates, but not at peripheral sensory and autonomic endings, explains why peripheral uptake of RABV is restricted to motoneurons after intramuscular inoculation in primates, rats, and guinea pigs (Tang et al., 1999; Graf et al., 2002; Ugolini et al., 2006; Ugolini, 2008, 2010, 2011), while sensory and sympathetic neurons that innervate the same muscle are not infected (Fig. 5) (section # 5.9.1). *In vitro*, RABV also binds a variety of other molecules (phospholipids, gangliosides, sialic acid, carbohydrates, heparin sulphate phosphoglycans, mGluR2), but their role as putative RABV (co)receptors *in vivo* remains unclear (Lafon, 2005; Guo et al., 2019).

5.4.2. Rabies virus internalization, retrograde axonal transport and replication

After G-mediated receptor binding, RABV is internalized by clathrin-mediated endocytosis (CME) (Gluska et al., 2014; Piccinotti and Whelan, 2016). Because CME mediates

internalization of the putative RABV receptors NCAM and p75NTR (Miñana et al., 2001; Butowt and von Bartheld, 2003; Guo et al., 2019), RABV may exploit both NCAM and p75NTR to highjack retrograde axonal transport mechanisms. RABV can be co-transported with p75NTR along axons (Gluska et al., 2014), but can also be transported without it, and transport of RABV is faster than p75NRT-mediated transport of nerve growth factor, suggesting that NCAM may be involved as well.

Retrograde axonal transport of RABV occurs at high speed. *In vivo*, we found that different groups of the same synaptic order located at various distances from first-order neurons (e.g., 10 µm to 2 cm) are infected at the same time (Ugolini, 2011). *In vitro*, the estimated transport speed varied among studies and cell types (50-100 mm/day in human DRG; Tsiang et al., 1991; 12-24 mm/day, Lycke and Tsiang, 1987, or 129 mm/day in rat DRG, Bauer et al., 2014; 8 mm/day in mouse neuroblastoma cells, Klingen et al., 2008). The fast retrograde axonal transport of RABV can only be explained by active axonal transport mechanisms (Ugolini, 2008, 2010, 2011) implicating dynein-mediated microtubule motors (Maday et al., 2014). It is inhibited by treatment with microtubule-disrupting drugs (Tsiang, 1979), and is specifically blocked by emetine (a translocation elongation inhibitor) by a mechanism that is not dependent on protein synthesis inhibition, probably involving emetine-induced decreased phosphorylation of dynein (MacGibeny et al., 2018).

During retrograde axonal transport, enveloped RABV particles are transported as cargo inside transport vesicles, and are released once they have reached the cell body (Klingen et al., 2008; Piccinotti and Whelan, 2016). The RABV G protein is crucial for highjacking specifically the retrograde axonal transport machinery, because it also confers retrograde axonal transport properties to pseudotyped lentiviruses (Mazarakis et al., 2001; Finke and Conzelmann, 2005) or VSV (Beier et al., 2013). The RABV P protein binds the dynein light chain LC8 (Jacob et al., 2000; Raux et al., 2000; Poisson et al., 2001) but is not required for axonal transport. Deletion or mutation of the P LC8-binding domain does not abrogate

transport of RABV from a peripheral site to the CNS (Tan et al., 2007) or axonal transport in DRG neurons *in vitro* (Bauer et al., 2014), but drastically attenuates primary transcription and replication (Mebatsion, 2001; Tan et al., 2007; Schnell et al., 2010), evincing a broader purpose of P-LC8 binding in regulating polymerase functionality and nucleocytoplasmic trafficking (Jespersen et al., 2019).

Replication takes place exclusively in the cytoplasm. Because the RABV genome consists of single-stranded RNA with negative sense polarity, it is first transcribed to produce complementary mRNA transcripts; transcripts must be translated into viral proteins before the viral RNA is replicated and new infectious particles are produced (Davis et al., 2015). The RABV P, N and M protein have important roles in regulating transcription and replication (Mebatsion, 2001; Tan et al., 2007; Schnell et al., 2010). The P protein, which is translated in five isoforms, interacts with the L, N and a multitude of host protein, and has multiples roles, including viral transcription, nucleocytoplasmic shuttling and evasion of cellular immunity, by inhibition of early interferon production and STAT signaling (Oksayan et al., 2012; Jespersen et al., 2019).

5.4.3. Budding and centrifugal intracellular transport of rabies virus

Both the M and G proteins play an important part in budding (Mebatsion et al., 1996a, 1999; Schnell et al., 2010); although the G is not essential for budding, in its absence RABV is released 30-fold less efficiently (Mebatsion et al., 1996a).

Centrifugal intracellular transport of molecules in neurons is polarized to dendrites or axons by different mechanisms (Nabb et al., 2020). No kinesin-binding motifs have been identified in any RABV protein (Guo et al., 2019). *In vivo,* centrifugal transport and budding of RABV is initially addressed only to dendrites, determining why transneuronal transfer occurs exclusively in the retrograde direction. It takes some time, as RABV immunolabeling initially involves the cell body and proximal dendrites, gradually extending to distal dendrites (Ugolini,

1995b, 2008, 2010) (Fig. 4 A-D). The time required for centrifugal transport to distal dendrites explains why a slight asynchrony of labeling of second-order populations may be detected in some systems (with delayed visualization of some populations that target exclusively distal dendrites) when RABV visualization is based on immunolabeling protocols that are not very sensitive (Ugolini, 1995b, 2008, 2010). Using very sensitive immunolabeling protocols, asynchronies are no longer observed (Ugolini et al., 2006), i.e., all populations of the same synaptic order are visualized simultaneously, including minor pathways (Ugolini et al., 2006) (Fig. 6 F), although initial differences in labeling intensity may be detected (Ugolini, 2010).

Anterograde axonal transport of RABV is inefficient *in vitro* in neuroblastoma cells (Klingen et al., 2008), but occurs at high speed (293 mm/day) in cultured DRG neurons in a glycoprotein-dependent manner, and is connected with vesicular transport (Bauer et al., 2014). Anterograde axonal transport of RABV can initiate 2 days after infection of DRG cell bodies *in vitro* (Bauer et al., 2014). Although RABV anterograde labeling of axons can also be detected i*n vivo,* it is temporally delayed compared with centrifugal transport to dendrites and does not lead to anterograde transneuronal transfer at the (asymptomatic) time points required for retrograde transneuronal tracing across multiple synapses (Ugolini, 2008, 2010). After intracortical injections, for example, anterograde transneuronal transfer of RABV from infected cortical neurons to the recipient (second-order) pontine nuclei does not occur even at 3 days (Fig. 7 A), when retrograde transneuronal transfer has already progressed to third-order neurons (Prevosto et al., 2009, 2010, 2011; Ugolini et al., 2019) (Figs. 7 and 8). Correspondingly, in human rabies (as well as in experimental studies of street RABV propagation, Murphy et al., 1973a,b), centrifugal transport and budding to end organs occurs only very late (e.g., at 6 days or longer, Murphy et al., 1973b), when the disease is already declared (Hemachudha et al., 2013), suggesting that it necessitates a considerable 'virus load' of neurons in order to occur (Ugolini, 2008, 2011; Hemachudha et al., 2013).

5.4.4. Mechanisms mediating neuronal integrity

Neurons infected with fully competent (and non-attenuated) RABV strains (section # 5.5.) show normal size and Nissl staining pattern (Ugolini 1995b; Tang et al., 1999) (Fig. 4 A-D) and remain metabolically viable after long standing infection, as they can express their neurotransmitters and transport other tracers (Ugolini, 2010) (section # 5.8). Cytopathic changes of infected CNS neurons are negligible even at the time of death in human rabies and apoptosis (programmed cell death) does not occur *in vivo* (Bertoune et al., 2017), because RABV has developed a multilevel strategy to preserve neuronal function (Hemachudha et al., 2013).

Firstly, RABV prevents activation of dendritic cells (antigen-presenting cells that have a key role in triggering innate and adaptive immune responses) (Huang et al., 2017) by replicating poorly at the peripheral site of inoculation (Hemachudha et al., 2013) and by expressing the G at low level to escape immune detection (Bertoune et al., 2017). The G expression level is modulated by the G itself by its cytoplasmic domain (Huang et al., 2017) as well as by selection of codon usage (Wirblich and Schnell, 2011). Secondly, RABV replication in neurons does not involve host shut off mechanisms (Rieder and Conzelmann, 2009). Thirdly, RABV prevents apoptosis of infected neurons *in vivo* (Bertoune et al., 2017), by keeping viral gene expression beyond threshold levels and actively interfering with pro-apoptotic factors (Morimoto et al., 1999; Finke and Conzelmann, 2005; Schnell et al., 2010; Hemachudha et al., 2013). Fourthly, RABV has developed other immunoevasive strategies that involve disrupting interferon signaling in infected neurons, via the P protein (Oksayan et al., 2012; Davis et al., 2015) and overexpressing immunosubversive molecules to inactivate 'protective' T lymphocites that invade the CNS in response to infection (Lafon, 2008).

5.5. Rabies virus strains: differences

There are two types of rabies virus strains: 'street' and 'fixed' ones. Street strains are natural isolates from infected animals or humans; their properties can be highly variable. 'Fixed' strains have been adapted from street RABV strains by repeated passages in rabbit and mice brains and cell culture, resulting in the selection of strains with stable properties (Wunner and Dietzschold, 1987; Morimoto et al., 1998). They are 100-10,000 times less infectious than 'street' strains (Dietzschold et al., 2005). Their prototype is the Challenge Virus Standard strain (CVS, originally employed as challenge virus to test the efficacy of rabies vaccines), that is used in transneuronal tracing studies, as well as in the construction of RABV recombinants. Several CVS subtypes are available, that differ in their passage history, such as CVS-11, CVS-24 and its B2c and N2c variants and CVS-26. The B2c and N2c variants were selected by passage in baby hamster kidney cells (BHK-21) (B2c) or mouse neuroblastoma cells (N2c) from a stock of the mouse-adapted CVS-24 that had been maintained exclusively in mouse brain for decades (Morimoto et al., 1998, 1999).

5.5.1. Differences in the G protein sequence of CVS strains

In view of the multiple roles of the G protein in receptor binding, internalization and intracellular cycle of RABV (section # 5.4), comparison of its genetic sequence in widely used strains of RABV is particularly relevant (Fig. 9). The CVS-11 strain used in our laboratory (Ugolini, 1995b; Ugolini et al., 2006) and in the other European institutions (e.g., Salin et al., 2008; Suzuki et al., 2012) comes from the CNRS (Gif sur Yvette, FR); it was originally obtained from P. Atanasiu (Institut Pasteur, FR) and is grown in BHK-21 cells (Seif et al., 1985). Its G protein is identical to the CVS of Yelverton et al. (1983). Comparison of its G protein sequence (accession n° 1106215A, Seif et al., 1985) with other CVS strains (Fig. 9) shows that it is very similar to the B2c CVS-24 variant from Philadelphia (n° AAB97691, Morimoto et al., 1998) (a difference of 3 amino acids, AA), and highly divergent from the "American" CVS-11 coming from the Center for Disease Control and Prevention in Atlanta, CDC (n° AAC34683, Smith et

al., 1973) (15 AA difference) and from the N2c CVS-24 variant (n° AAB97690, Morimoto et al., 1998) (11 AA) (Fig. 9). Such differences involve specifically the G external domain (which is involved in receptor-mediated internalization). Thus, they may underlie conformational changes and modify receptor binding affinity and virus internalization rate, which could explain some differences in properties of these CVS strains (section # 5.9.4).

The similarity between the 'French' CVS-11 (denominated here CVS-11 FR) and B2c (a difference of only 3 AA) and their major divergence from N2c (11 AA) are notably correlated with differences in the way these viruses have been selected and maintained. N2c was selected in neuroblastoma cells, whereas B2c and CVS-11 FR (both grown in BHK-21 cells) are very close to the original CVS-11 that had been adapted several decades ago from mouse-brain passaged CVS (which differs from B2c only in 2 AA of the G sequence, Morimoto et al., 1998, 1999). Curiously, CVS-11 from the CDC (CVS-11 CDC) is highly divergent from CVS-11 FR (15 AA difference, Fig. 9), suggesting a different passage history. Comparison of genome sequences and neutralizing monoclonal antibody analysis of fixed RABV strains revealed major discrepancies with their recorded lineage, reflecting substantial faults in recorded history (Lafon et al., 1988; Sacramento et al., 1992; Smith et al., 1992).

5.5.2. Differences between attenuated strains (such as SAD B19) and more pathogenic RABV strains (such as CVS)

The *attenuated* SAD B19 strain of RABV has been included in Fig. 9 because it is widely employed as virus backbone for construction of defective RABV recombinants (section # 6). Its G sequence (accession n° M31046.1, Conzelmann et al., 1990) highly diverges from all CVS strains, both in the G external domain and in the cytoplasmic domain (Fig. 9), which has a multifunctional role, notably in determining virus expression level and actively promoting neuronal survival (section # 5.4). SAD B19 displays differences in other regions of the virus genome as well (Conzelmann et al., 1990; Smith et al., 1992).

Attenuated RABV strains, such as SAD B19 and derived recombinants, are significantly less neuroinvasive; protective microglial response is less pronounced (Bertoune et al., 2017). Differences between attenuated and more pathogenic RABV strains (such as CSV) are determined by the genetic sequence and expression level of their G, as well as by the M and P proteins (Schnell et al., 2010; Bertoune et al., 2017). Compared with more pathogenic RABV strains, attenuated strains overexpress the G and show a more pro-apoptotic phenotype *in vitro*, but not *in vivo* (Bertoune et al., 2017). Importantly, SAD B19 and related chimeric recombinants display a higher rate of viral transcription and proteins expression per neuron, causing viral burden of individual neurons which may impair neuronal functioning, finally cumulating in cell death (Bertoune et al., 2017) (section # 6).

5.6. Identification of the synaptic order: kinetics of transfer

Using CVS-11 FR, we have demonstrated that RABV behaves in a consistent fashion in primates and rodents. Using virus stock at high titer (at or above 10^{10} PFU/ml) and keeping the amounts constant is very important to avoid variability; high virus concentrations guarantee 100% infectivity and maximize transneuronal transfer (Ugolini, 2010).

Studying the kinetics of transfer at different time points after the injections is of paramount importance for identifying the order of connections. Transneuronal transfer is strictly time dependent. Regardless of whether RABV is injected peripherally on directly into the CNS, labeling of first-order neurons requires 2 days; subsequent retrograde transneuronal labeling of second-order, third-order and higher-order neurons occur stepwise at regular intervals (12 hours or more, depending on the system and the viral load) (Ugolini, 1995b, 2008, 2010, 2011; Tang et al., 1999; Graf et al., 2002; Grantyn et al., 2002; Morcuende et al., 2002; Moschovakis et al., 2004; Ugolini et al., 2006, 2019; Prevosto et al., 2009, 2010, 2011, 2017) (Figs. 6-8). In monkeys, for example, after injections of CVS-11 FR (10^{10} PFU/ml) into eye muscles (110 µl) (Ugolini et al., 2006; Prevosto et al., 2017) or into the posterior parietal

cortex (2 µl) (Prevosto et al., 2009, 2010, 2011; Ugolini et al., 2019), labeling involves only first-order neurons at 2 days, and higher-order neurons are labeled stepwise at 12 hrs intervals (Ugolini, 2010) (Figs. 6-8). Stepwise visualization of successive synaptic relays is determined by the time required for each viral replication cycle in recipient neurons. The distance does not influence the speed of visualization of different pathways of the same order (short pathways are labeled at the same time as long ones) (Ugolini et al., 2006; Ugolini, 2010, 2011). The reason is that axonal transport occurs at very high rate, and RABV replication in recipient neurons takes much longer, 'canceling out' differences in tracer accumulation that may result from transport distances (Ugolini, 2008, 2010, 2011).

5.7. Unidirectional transfer of RABV at chemical synapses

Transneuronal transfer of RABV occurs unidirectionally also after intracortical injections (Figs. 7 A and 8) (Prevosto et al., 2009, 2010, 2011; Ugolini et al., 2019). Uptake by fibers of passage or local spread do not occur (Fig. 4 D,G,H) (Ugolini 1995b, 2010). In all models that we have investigated, transneuronal transfer of RABV has never failed to label known pathways mediated by classical chemical synapses ('wiring transmission') regardless of their neurotransmitters, including also minor pathways (e.g., Ugolini, 1995b, 2010; Tang et al., 1999; Graf et al., 2002; Morcuende et al., 2002; Grantyn et al., 2002; Ugolini et al., 2006). Only 'volume transmission' pathways (Fuxe et al., 2007), might be less conducive to RABV compared to alpha-herpesviruses (Ugolini, 1995b, 2010; Tang et al., 1999).

We found that RABV does not propagate via gap junctions, as infected bulbospongiosus (BS) motoneurons, which are interconnected by gap junctions, do not increase in number with time (Tang et al., 1999) (Fig. 10). Conversely, BS motoneurons infected with Bartha PrV progressively become more numerous (Marson and McKenna, 1996), probably because of spurious spread of PrV. Similarly, inferior olive (IO) neurons, which are linked by gap junctions, are heavily infected by local spread of HSV 1 from

hypoglossal axons (Ugolini et al., 1987) (Fig. 2 C,D), which does not occur with RABV (Ugolini, 1995b) (Fig. 4 D).

5.8. Combined visualization of RABV with other tracers, neurotransmitters or cell markers

Using sensitive immunoperoxidase protocols, RABV immunolabeling is Golgi-like, revealing the finest arborization of labeled neurons, and can be routinely combined with cresyl violet counterstaining (Ugolini et al., 2006, 2019; Ugolini 2010) (Figs. 6-8). Because infected neurons remain metabolically viable, they express their neurotransmitters and can transport other tracers (although not all tracers are suitable, Ugolini, 2010). Published protocols for dual color visualization of RABV transneuronal labeling and neurotransmitter or cell markers describe the combined visualization of RABV and choline acetyltransferase (to identify motoneurons and autonomic preganglionic neurons) (Graf et al., 2002; Morcuende et al., 2002; Tang et al., 1999; Ugolini et al., 2006) (Fig. 6 B-E), oxytocin (Tang et al., 1999), the N-terminal region of tryptophan hydroxylase-2 (to identify serotoninergic neurons, Rice et al., 2009), as well as glycine, calbindin, parvalbumin, pleiotrophin and neuronal nitric oxide synthase (Miyachi et al., 2006; Salin et al., 2009; Coulon et al., 2011).

For dual tracing purposes, retrograde transneuronal labeling with RABV has been successfully combined with labeling of neurons innervating another target using the conventional retrograde tracers Fluoro-Ruby (Morcuende et al., 2002) or Fluoro-Gold (Rice et al., 2010), to determine whether the same neurons have collateralized projections to both targets. Other protocols involve the combination of retrograde transneuronal tracing with RABV with multiple anterograde tracers such as Phaseolus vulgaris-leucoagglutinin and biotinylated dextran amine (Salin et al., 2008; López et al., 2010).

We have demonstrated that it is possible to inject a mixture of rabies virus and the conventional tracer cholera toxin B fragment (CTB, end concentration 0,03%) without altering

the uptake of either tracer (Prevosto et al., 2009, 2010, 2011; Ugolini et al., 2019). This tracer combination is highly valuable, as it makes it possible to visualize in the same experiment the injection area, as well and direct projections (first-order neurons) with CTB (Fig. 7 A-C)., in combination with transneuronal labeling of higher-order neurons with RABV (Fig. 7 A and D-H). The simultaneous identification of first-order neurons (CTB) and higher-order neurons (RABV) is a major advantage. Importantly, CTB immunolabeling allows for a precise definition of the injection site, which is difficult using RABV alone because the rabies tracer does not accumulate at the injection site and does not label glial cells, and transneuronal labelling can include short-distance projection neurons (Prevosto et al., 2009, 2010, 2011; Ugolini, 2010; Ugolini et al., 2019) (Fig. 7 C,D). This CTB-RABV combination has been successfully adopted by other investigators as well (e.g., Coffman et al., 2011; Suzuki et al., 2012; Jwair et al., 2017).

The properties of RABV rabies as a transneuronal tracer, described here, refer specifically to the French CVS-11 FR subtype (similar to B2c CVS-24, see above), which is the only RABV strain used in European laboratories and is the CVS strain of which uptake and transneuronal tracing properties have been most thoroughly evaluated (Ugolini, 1995b; Tang et al., 1999; Graf et al., 2002; Morcuende et al., 2002; Grantyn et al., 2002; Moschovakis et al., 2004; Ugolini et al., 2006, 2019; Prevosto et al., 2009, 2010, 2011, 2017). Other CVS strains (CVS-11 CDC, 26, B2c, N2c) share the unidirectional transport properties of CVS-11 FR (Kelly and Strick, 2000), but may propagate at different rates and differ in other properties as well (section # 5.9.4). Thus, when using a particular RABV strain for retrograde transneuronal tracing, the transport efficiency of each strain should be evaluated in test models, and the kinetics of virus propagation should be studied to determine the time required for each synaptic step.

5.9. Peripheral uptake of rabies virus and differences related to host species and virus strains

5.9.1. RABV is the ideal tracer to study motor innervation: methodological aspects

After peripheral inoculations, the probability of entry of RABV in terminals is low, because RABV does not replicate well in non-neuronal tissue. RABV lies in the muscle as a smoldering infection, that remains confined to the injected portion of the muscle (Ugolini, et al., 2006; Hemachudha et al., 2013) (Fig. 6). This explains why local infiltration of the wound with rabies immunoglobulins effectively prevents the infection if done early after exposure (Ugolini, 2011).

RABV is the ideal transneuronal tracer for studying motor networks (and the only viral transneuronal tracer available for this purpose), as it enters exclusively at motor endplates after intramuscular injections in rats, guinea pigs and primates (Tang et al., 1999; Graf et al., 2002; Ugolini et al., 2006; Rathelot and Strick, 2006) (Figs. 5, 6 and 10) (see also # 5.4.1). It makes it possible to unravel with great specificity polysynaptic motor pathways involved in the control of single muscles**.**

Because RABV does not diffuse in the muscle (Ugolini et al., 2006), it is important inject the same portion of the muscle in a series of experiments, to ensure the same amount of uptake. Exploiting this property of RABV, we were able to label selectively, in primates, the motoneuron populations that supply slow (multiply innervated, MIF) and fast (singly innervated, SIF) muscle fibers, by injecting CVS-11 FR into either the distal or central portion of the lateral rectus (LR) muscle (Ugolini et al., 2006) (Fig. 6). After distal injections (Fig. 6 A), uptake involved exclusively MIF motoneurons located at the periphery of the abducens nucleus (Fig. 6 G). In contrast, SIF motoneurons (located inside the abducens nucleus, Fig. 6 H) were infected only after injection into the center of the muscle belly, i.e., the only portion of the LR muscle containing the ‘en plaque’ endplates of these motoneurons (Fig. 6 A-C). Transfer of RABV revealed major differences in monosynaptic and polysynaptic innervation of these distinct motoneuron populations (Ugolini et al., 2006; Prevosto et al., 2017) (Fig. 6).

Peripheral entry via the motor route is not an exclusive property of the "fixed" CVS strain: when classic experimental studies of street RABV propagation (Murphy et al., 1973a,b; Murphy & Bauer, 1974; Charlton et al., 1996) are revisited taking into account current knowledge on CNS connectivity, the early propagation properties of street RABV strains to the spinal cord and brain seem to be indistinguishable from those of fixed RABV (CVS), and consistent with uptake via the motor route and retrograde transneuronal transfer (to propriospinal and descending pathways) (Hemachudha et al., 2013). An exception might be some *bat* RABV variants, which are able to multiply in epidermal cells *in vitro* (Morimoto et al., 1996), unlike other street or fixed RABV strains. Human rabies associated with bat variants is characterized by much higher incidence of neuropathic pain, as well as Horner's syndrome and other *atypical* features, which might suggest additional (or alternative) transmission via sensory or sympathetic skin innervation (Ugolini, 2011; Hemachudha et al., 2013).

5.9.2. Centrifugal transport to sensory ganglia is mediated by retrograde transneuronal transfer

In rats, guinea pigs and primates, primary sensory neurons (in trigeminal ganglion and DRG) are not involved by peripheral uptake of RABV (CVS-11 FR) after intramuscular injection (Figs. 5 A and 10 A), but can be infected via their central (spinal) connections, by retrograde transneuronal transfer of RABV from motoneurons and connected premotor interneurons (Tang et al., 1999; Ugolini 2008, 2011) (Fig. 10 A). Similarly with street RABV, inoculations into limb muscles lead to early infection of spinal motoneurons and intermediate zone interneurons (and sparing of the dorsal horn); DRG infection involves mainly large and medium-size neurons, first ipsilaterally at segmental levels, and later bilaterally and at additional levels (Charlton et al., 1996), consistent with DRG connections to retrogradely infected spinal motoneurons and interneurons. Other examples of infection of sensory

ganglia that is mediated by retrograde transneuronal transfer of RABV (CVS-11 FR) is the labeling of the vestibular (Scarpa's) ganglia, which reflects polysynaptic inputs to eye muscles motoneurons (Graf et al., 2002; Ugolini et al., 2006) (Fig. 5 C) or to the posterior parietal cortex area MIP (i.e., ascending trisynaptic pathways from Scarpa's ganglia to vestibulothalamic neurons and then thalamocortical neurons) (Ugolini et al., 2019, Figs. 7 H, 8).

Infection of sensory ganglia that is mediated by retrograde transneuronal transfer of RABV from motoneurons has a major role in human rabies pathophysiology, as long-standing infection ultimately triggers immune attack of the infected DRG, explaining local prodromal symptoms and signs that occur only at disease onset, after a very long incubation period (see Hemachudha et al., 2013). Retrograde transneuronal involvement of DRG also explains late-occurring centrifugal spread of RABV to extraneural organs, because all extraneural organs in which RABV can be recovered receive sensory innervation (Hemachudha et al., 2013).

5.9.3. Additional sensory uptake in mice.

With regard to peripheral uptake, mice are a special case, because intramuscular inoculations of CVS or its avirulent variants lead to simultaneous uptake by motoneurons and primary sensory neurons (Coulon et al., 1989, 2011; Jackson, 1991; Tuffereau et al., 2007). This property must be taken into account when transneuronal tracing studies are performed in mice. Direct sensory uptake from the muscle as well as transneuronal transfer can similarly explain infection of proprioceptive DRG obtained in neonatal mice with monosynaptically restricted RABV-based technology (Stepien et al., 2010) (section # 6). The additional sensory uptake of CVS strains in mice (but not in other rodent species or primates) is likely due to the fact that all CVS strains are mouse-adapted (as they were passaged in mice brains over centuries, Sacramento et al., 1992). Thus, mouse models are less representative of RABV

infection than other rodents and primates (Ugolini, 2008, 2010, 2011), when using mouse-adapted CVS strains.

Sensory uptake of RABV in mice involves only specific DRG subpopulations, i.e., large-diameter (myelinated), capsaicin-insensitive neurons, that include proprioceptive DRG, both *in vivo* and in primary culture (Tuffereau et al., 2007). Thus, in mice, RABV is the specular image of alpha-herpesviruses, which preferentially infect small-diameter DRG neurons after intramuscular inoculations (Ugolini, 1992, 2010, 2011) (Fig. 3). Remarkably, lack of infection of unmyelinated (small diameter) DRG neurons (nonpeptidergic and tyrosine hydroxylase positive) was also reported after intraspinal injection of RABV recombinants from SAD B19 lacking the G gene, and pseudotyped with the G of SAD or N2c (Albisetti et al., 2017). It reflects impaired internalization, because the same DRG subtypes can support RABV replication if the G-mediated entry is bypassed by pseudotyping the recombinants with another surface protein (Albisetti et al., 2017).

5.9.4. A special case: the N2c variant of CVS-24

Available studies indicate four major differences of N2c compared with CVS-11 FR and the other CVS strains: a higher transfer rate, variability after peripheral inoculations, uptake involving also autonomic neurons in some conditions, and a certain asynchrony in the visualization of populations of the same synaptic order.

Firstly, N2c propagates much more rapidly than the other CVS strains after peripheral or CNS inoculations. It was detected in cortical neurons 1-2 days before CVS-26 after intramuscular inoculations in primates (Kelly and Strick, 2000; virus stock titers and inoculum volumes were not indicated). Similarly, after CNS injection of N2c (0.2-0.6 µl; Hoshi et al., 2005) or CVS-11 CDC (4.4-11.4 µl; Kelly and Strick, 2003) using virus stocks of *equal* concentration (1.7×10^7 PFU/ml), second-order neurons are already labeled at 40 hrs with N2c (versus 3 days with CVS-11 CDC) and third-order labeling is obtained at 50 hrs with N2c

(versus 4 days with CVS-11 CDC). N2c also propagates much more rapidly that CVS-11 FR at equal distances, although CVS-11 FR is used at higher concentration (at or above 10^{10} PFU/ml), both after CNS injection (e.g., CVS-11 FR: 5.96 x 10^{10} PFU/ml; 2 µl; Ugolini et al., 2019) and peripheral inoculation (N2c: 1-5 x 10^9 PFU/ml; 130-170 µl, ciliary body: May et al., 2018; CVS-11 FR: 7.8 x 10^{10} PFU/ml; 110 µl, eye muscles: Ugolini et al., 2006; Prevosto et al., 2017). With N2c, 10^7 PFU/ml seems sufficient for maximizing N2c infectivity, as second-order labeling equally occurs at 42 hrs using virus stocks at 1.7 x 10^7 PFU/ml (0,2-0.6 µl; Hoshi et al., 2005) or 4.5 x 10^9 PFU/ml (9-11.8 µl; Bostan et al., 2010).

Secondly, variability of the results was reported after peripheral inoculations using N2c batches at the same titer (1x $10^{7.7}$ PFU/ml; 0.25 -1.5 ml; Rathelot and Strick, 2009), that we never experienced with CVS-11 FR (7.8 x 10^{10} PFU/ml; 110 µl; e.g., Ugolini et al., 2006; Prevosto et al., 2017). Major variability occurs after injections of N2c into other extraneural organs (1x 10^8 or 4.5x 10^9 PFU/ml; 14-16 µl, kidney: Levinthal and Strick, 2012; 5 x 10^8 PFU/ml; 80-100 µl, adrenal medulla: Dum et al., 2016), so that the survival time, by itself, is not sufficient to define the synaptic order in any experiment (Dum et al., 2016). Instead, the distribution of labeled neurons within well- known pathways must be used as internal controls.

Thirdly, N2c can propagate in autonomic pathways in some conditions. Uptake and transneuronal transfer of N2c in *parasympathetic* pathways was obtained after injection into the ciliary body in macaque monkeys (1-5 x 10^9 PFU/ml; 130-170 µl; May et al., 2018). Infection of *sympathetic* pathways was reported after N2c injections into the kidney or adrenal medulla in rat and monkeys (1x 10^8 or 4.5x 10^9 PFU/ml; 14-16 µl; Levinthal and Strick, 2012; 5 x 10^8 PFU/ml; 80-100 µl; Dum et al., 2016). In those studies, N2c infection of sympathetic preganglionic cell group and spinal intermediate zone occurred at the putative third-order time point (Levinthal and Strick, 2012); disynaptic time points were not studied, and most experiments involved very long time points (78-134 hrs, or 97-136 hrs) consistent

with putative forth- to sixth-order labeling. By contrast, sympathetic uptake does not occur after injection of N2c into the ciliary body (1-5 x 10^9 PFU/ml; 130-170 µl; May et al., 2018) or after intramuscular inoculations (1.7 x $10^{7.7}$ PFU/ml; 0.25-0.5 ml; Rathelot and Strick, 2006). In the latter case, N2c infects only motoneurons (Rathelot and Strick, 2006), like CSV-11 FR (3.9 x 10^{10} PFU/ml; 2 µl; Tang et al., 1999; 7.8 x 10^{10} PFU/ml; 110 µl; Ugolini et al., 2006) (Figs. 5 A and 10 A).

Fourth, intramuscular injection of N2c resulted in asynchronous visualization of population of the same synaptic order (1.7 x $10^{7.7}$ PFU/ml; 0.25-0.5 ml; Rathelot and Strick, 2006). Some asynchrony also occurred during transfer of N2c from the ciliary body (1-5 x 10^9 PFU/ml; 130-170 µl; May et al., 2018), that we did not experience with CVS-11 FR at equivalent distances (7.8 x 10^{10} PFU/ml; 110 µl; Ugolini et al., 2006; Prevosto et al., 2017).

How to explain these puzzling differences? These peculiar properties of N2c are likely due to the way it was selected. Because of a high mutation rate, RNA viruses like RABV usually consist of complex populations (quasispecies) (Morimoto et al., 1998). The N2c variant of CVS-24 was selected by passage in neuroblastoma cells, which selectively enhances replication of the most neurovirulent variant in a quasispecies complex (Morimoto et al., 1998), and facilitates random back-mutation of attenuated RABV (Clark, 1980). Unlike B2c and CVS-11 (Ugolini, 1995b), N2c does not grow well in non-neuronal cells *in vitro* and *in vivo* (Morimoto et al., 1998). This is important, because the probability of entry of RABV in nerve endings is intrinsically low after peripheral inoculations, and low-level replication in non-neuronal tissue at the peripheral inoculation site augments local virus concentration, increasing the likelihood of incorporation by terminals (Hemachudha et al., 2013). Thus, the inability of N2c to replicate in non-neuronal tissue can explain why a major variability of the results can occur after peripheral inoculations of N2c, but not CVS-11 FR (see above).

The faster propagation of N2c is probably due to higher internalization efficiency (e.g., Faber et al., 2004), whereas differences in axonal transport rate are unlikely (as all CVS strains

hijack the same axonal transport machinery). A higher internalization efficiency of N2c may also *desynchronize* the visualization of populations of the same synaptic order if they differ in distance, synaptic strength or site of terminations on the transferring neurons (Ugolini, 2010), explaining some asynchrony with N2c. Distinction of the synaptic order is much easier using CVS-11 FR.

The G external domain of N2c highly diverges from that of B2c or CVS-11 FR, that are grown in BHK-21 (Fig. 9). Adaptation to neuroblastoma cells of N2c may also explain why only this particular RABV variant can infect autonomic pathways in some conditions. Importantly, neuroblastoma cells are thought to be derived from postganglionic sympathetic neuroblasts, and possess a variety of phenotypic characters of differentiated neurons, including muscarinic receptors expression (Thiele et al., 1998). Thus, growing N2c in neuroblastoma cell lines may have conferred to its G protein the ability to bind putative receptors of parasympathetic postganglionic neurons, possibly including muscarinic acetylcholine receptors expressed on the innervated tissue (ciliary body). The puzzling findings that N2c can infect sympathetic pathways after injection into the kidney or adrenal medulla, but not after injection into the ciliary body or muscles (see above) may be explained by hypothesizing a low (albeit present) affinity of N2c for sympathetic ending. In this case, some uptake of N2c can occur when such terminals are sufficiently numerous in the injected organ (kidney, adrenal medulla), but not when they are few (sympathetic innervation of the ciliary body, Ruskell 1973; May et al., 2018). However, if the targeted organ receives *also* motor innervation (muscle), high affinity binding of the G to nAChR at motor endplates prevails over low affinity binding to putative receptors at sympathetic endings (where nAChr are not present). This would explain why N2c infects only motoneurons after intramuscular injections, like CVS-11 FR (see above), despite the major sympathetic innervation of striated muscles and the vicinity of sympathetic terminals to motor endplates (Rudolf and Straka, 2019). In other words, even N2c retains a preferential tropism for motoneurons.

6. Genetically modified rhabdovirus tracers

When molecular cloning of RABV became possible (Schnell et al., 1994; Conzelmann, 1996), virologists generated chimeric viruses by exchanging viral genes between pathogenic and attenuated RABV strains to study the role of individual genes in pathogenicity. This technology has provided outstanding opportunities to engineer modified RABV tracers that carry reporter genes and can be tailored for specific purposes. The neuroscientist toolbox currently includes multiple chimeric viral tools that propagate either anterogradely or retrogradely and function either as single step tracers or monosynaptically restricted tracers, or serve for monitoring and manipulating neuronal activity and gene expression.

6.1. Defective RABV as single step tracer

The first step was generation of a RABV recombinant from the attenuated SAD-B19, where the G protein gene was deleted (dG) (Mebatsion et al., 1996a). This SAD-dG recombinant was then pseudotyped (equipped) with the G of RABV by trans-complementation (growing it in cells that express the G) (Etessami et al., 2000), so that it is internalized via the G and replicates in first-order neurons, but cannot propagate further, because progeny virus lacks the G. Insertion of marker genes in the RABV genome was another major achievement (Mebatsion et al., 1996b). Combining these approaches led to the introduction of the first *defective* (G-deleted) RABV-dG tracer carrying a transgene as marker, which behaves like a *single step* (retrograde) tracer because it cannot cross synapses, and provides intense labeling due to RABV replication and transgene expression (Wickersham et al., 2007a).

6.2. Monosynaptically restricted RABV tracers

Defective (RABV-dG) recombinants can be pseudotyped in different ways, either with the G protein of RABV or VSV, or with the surface glycoprotein of another virus (the avian retrovirus glycoprotein EnvA). When pseudotyped, RABV-dG viruses behave as *monosynaptically restricted transneuronal tracers*, as they can cross only one synapse.

Because the receptor for EnvA (TVA) is not expressed in mammals, the purpose of pseudotyping RABV-dG recombinants with EnvA is to identify direct connections to selected cell types or single neurons, that are specifically targeted by making them to express both the appropriate avian receptor TVA (so that the recombinant carrying ENVA can enter the cell), and the RABV G, necessary for pseudotyping RABV-dG *in vivo* (Wickersham et al., 2007b). Thus, progeny virus is trans-complemented with the RABV G protein in first-order neurons, and is transferred to presynaptic (second-order) neurons, but cannot propagate further. Initial targeting attempts made use of the 'gene gun' technique in brain slices (Wickersham et al., 2007b).

Targeting possibilities *in vivo* involve the use of cell type-specific Cre drivers, necessitating availability of mouse lines that express Cre recombinase in the cell types of interest (Callaway and Luo, 2015). Alternatively, RABV-dG can be pseudotyped with the RABV G protein using a helper virus (an adeno-associated virus expressing the RABV G, AAV-G) to deliver the RABV G protein to first-order neurons, either by prior injection (e.g., Reardon et al., 2016), or by co-injecting into the same muscle AAV-G and the defective RABV-dG (where the G gene is replaced by a reporter gene). Progeny virus is pseudotyped with the RABV G protein, can bud from first-order neurons and is transferred only to second-order neurons (Stepien et al., 2010; Tripodi et al., 2011). For data interpretations in mouse models, simultaneous RABV peripheral uptake by motor and DRG neurons should be taken into account (see # 5.9.3).

Although monosynaptically restricted transneuronal tracing using RABV-dG recombinants is often advocated as 'the' alternative to the use of fully competent RABV for

polysynaptic transneuronal tracing, it is important to understand that the two technologies serve complementary purposes. Using RABV recombinants provides additional possibilities, but does not replace polysynaptic transneuronal tracing with fully competent RABV (CVS). When RABV polysynaptic transneuronal tracing is correctly applied (section # 5), the ability of wild-type RABV to cross multiple synapses stepwise, at distinct intervals, does not create 'potential confounds in interpretations' (as stated by some investigators), and is a major advantage in connectomic studies. Indeed, only fully competent RABV allows for a comprehensive mapping, step by step, of the entirety of functional neuronal networks converging, for example, upon a single muscle or a given cortical area, including second-order, third-order and even higher order populations if required (Figs. 6-8). This cannot be achieved using monosynaptically restricted transneuronal tracing with RABV-dG viruses, which can serve to identify only second-order neurons, and may not even label all second-order populations (Callaway and Luo, 2015) (see # 6.3 and 6.4).

6.3. Properties of RABV-dG tracers differ depending upon the pseudotyping protocol and backbone virus

It is important to know that the properties of pseudotyped RABV-dG tracers are not equivalent to that of virulent RABV strains, for two reasons. Firstly, cellular tropism, uptake and transport direction are determined by the supplied glycoprotein, as RABV-dG recombinants pseudotyped with the VSV G are transported anterogradely, like VSV (Haberl et al., 2015), and VSV-dG pseudotyped with the G of RABV is transported retrogradely, like RABV (Beier et al., 2013). Similarly, cellular tropism and propagation of a RABV-dG tracer that is targeted to a given cell type using the EnvA-TVA system (e.g., Zampieri et al., 2014) is not representative of the behavior of RABV *in vivo*.

Secondly, transgene expression level and cytotoxicity crucially depend upon the backbone virus (and its interaction with the supplied surface protein, see # 5 and 6.6). All first

generation recombinants were constructed from *attenuated* RABV strains (SAD B19 or HEP-Flury) or VSV as virus backbone, because of their high-level expression of transgenes. A drawback is that attenuated RABV and VSV strains are weakly neurotropic, highly immunogenic and cytotoxic, albeit with major differences (see # 5.2, 5.3 and 5.5.2). With attenuated VSV-dG, transgene expression is detectable within 1 hour, but physiological recordings are restricted to less than 1 day and severe, fast-onset cytotoxicity begins within 1-2 days even with attenuated (less cytotoxic) M51 variants of VSV-dG (Van den Pol et al., 2009; Beier et al., 2011). With SAD B19-dG, transgene expression is detectable from 2 days, electrophysiological properties are preserved for 12 days, and cell loss occurs after 14 days (Wickersham et al., 2007a; Osakada et al., 2011; Callaway and Luo, 2015). Similarly, with HEP-Flury-dG, the basic properties of neurons can be maintained only for 16 days (Ohara et al., 2013b, 2017), due to the viral burden induced by high-level replication of attenuated RABV strains (Bertoune et al., 2017) (# 5.5.2). A self-inactivating dG-RABV that transcriptionally disappears from the infected neurons is a promising tool for long-term functional and genetic modification of neural networks (Ciabatti et al., 2017).

6.4. Second-generation RABV recombinants with higher transfer efficiency

Another important limitation of first generation, SAD B19-derived tracers is that they label only a fraction of presynaptic neurons (Callaway and Luo, 2015). A limiting factor is that they are pseudotyped with the G protein from SAD B19, which contains mutations responsible for reduced internalization (see section # 5.5.2). Major improvement in transfer efficiency has been obtained by pseudotyping SAD B19-dG with a codon-optimized chimeric G protein consisting of the transmembrane/cytoplasmic domain of SAD B19 G and the G extracellular domain of the pathogenic Pasteur virus strain (Kim et al., 2016). An alternative, successful approach involved generation of CVS N2c-based recombinants (Reardon et al., 2016). Direct comparison with the first generation SAD B19-dG recombinant showed that CVS

N2c-dG exhibits at least an order of magnitude enhancement in transneuronal transfer to presynaptic neurons, particularly over long distances, while keeping neurons viable for a longer period *in vitro* and *in vivo* (Reardon et al., 2016). Predictably, transgene expression directed by N2c-dG (virulent virus backbone) takes longer to be detectable and is lower, but is sufficient to enable monitoring neuronal activity with calcium indicators and optogenetic manipulation for up to 28 days (Reardon et al., 2016). Because these second-generation recombinants (Kim et al., 2016; Reardon et al., 2016) differ both in backbone virus (SAD B19 strain versus CVS N2c) and surface domain (PV versus N2c) of the RABV G protein used for pseudotyping them, a direct comparison in the same system would be required to determine their relative transfer efficiency, and clarify potential G-mediated differences in uptake.

6.5. Dual monosynaptic tracing opportunities

Available viral tools for monosynaptically restricted *anterograde* tracing studies are SAD B19-dG viruses pseudotyped with a chimeric G protein, containing the external (receptor-binding) domain of the VSV G, to confer anterograde transport properties, and the transmembrane and cytoplasmic domain of the native RABV G (Haberl et al., 2015). Due to the VSV G external domain, this chimeric recombinant has a strong bias for excitatory (versus inhibitory) neurons and also infects glial cells (Haberl et al., 2015, 2017). Properties conferred by the SAD B19 backbone are high-level transgene expression and lower cytotoxicity (Haberl et al., 2015) compared with recombinants where VSV is the virus backbone (Beier et al., 2011, 2013). Different reporter genes can be inserted in isogenic RABV-derived recombinants to enable monosynaptically restricted dual anterograde tracing (Haberl et al., 2015, 2017) or retrograde tracing (Tripodi et al., 2011). It may be also possible to combine directionally opposite RABV-based tracers to simultaneously label projections to and from the injection site. VSV-based recombinants are also available (Beier et al., 2011, 2013), albeit hampered by major VSV cytotoxicity (# 5.3 and 6.3). When co-injected, VSV-based recombinants infect

different cells even at the injection site (Beier et al., 2013); their inability to infect the same cell indicates major viral interference for replication, probably due to high-level replication of VSV.

6.6. Dual polysynaptic retrograde transneuronal tracing with RABV isogenic recombinants

Because of the strictly unidirectional transfer of RABV and its specificity, dual *polysynaptic* retrograde transneuronal tracing tools based on isogenic RABV strains are highly desirable. Multiple isogenic RABV recombinants were generated by inserting different reporter genes in the highly attenuated HEP-Flury strain, and replacing the parental G with the G gene from the virulent CVS strain, in order to mimic the properties of CVS (Ohara et al., 2009a,b). As these chimeric RABV recombinants are fully competent for uptake and replication, they successfully enable dual retrograde transneuronal tracing across multiple synapses (Ohara et al., 2009a,b, 2013a). Their transfer efficiency has not been compared with that of CVS. For successful dual infection, the two viruses must reach the same cell within a few hours, otherwise the first virus can preclude replication of the other virus (Ohara et al., 2009a,b, 2013a). Thus, negative dual labeling results should be interpreted conservatively. The same considerations apply to dual labeling with PrV strains (Enquist and Card, 2003; section # 4.5). HEP-Flury recombinants that carry the G gene of CVS must be visualized immunohistochemically (Ohara et al., 2009a, 2013a) because they display low transgene expression, compared with G-deleted HEP-Flury (Ohara et al., 2013b). Increased transgene expression, with efficient transneuronal transfer, was recently obtained by enhancing activity of the viral RNA-polimerase L, by deleting the extra transcription unit and shortening the intergenic region between the G and L genes (Ohara et al., 2017). Inserting as transgene a fluorescent timer that changes color with time cannot perfectly differentiate first-order from second-order neurons (Ohara et al., 2017). To distinguish first-order neurons, co-injecting

RABV-derived tracers and CTB would be a reliable approach (Prevosto et al., 2009, 2010; see section # 5.8).

Acknowledgements

This work was supported by the European Union (QLRT-2001-00151, EUROKINESIS, and BIO4-CT98-0546, TransVirus) and the Centre National de la Recherche Scientifique (CNRS).

References

Albisetti, G.W., Ghanem, A., Foster, E., Conzelmann, K.K., Zeilhofer, H.U., Wildner, H., 2017. Identification of Two Classes of Somatosensory Neurons That Display Resistance to Retrograde Infection by Rabies Virus. J. Neurosci. 37, 10358-10371.

Alstermark, B., Kümmel, H., 1990. Transneuronal transport of wheat germ agglutinin conjugated horseradish peroxidase into last order spinal interneurones projecting to acromio- and spinodeltoideus motoneurones in the cat. 1. Location of labelled interneurones and influence of synaptic activity on the transneuronal transport. Exp. Brain Res. 80, 83-95.

Alstermark, B., Kümmel, H., Tantisira, B., 1987. Monosynaptic raphespinal and reticulospinal projection to forelimb motoneurones in cats. Neurosci. Lett. 74, 286-290.

Aston-Jones, G., Card, J.P., 2000. Use of pseudorabies virus to delineate multisynaptic circuits in brain: opportunities and limitations. J. Neurosci. Methods 103, 51-61.

Babic, N., Klupp, B., Brack, A., Mettenleiter, T.C., Ugolini, G., Flamand, A., 1996. Deletion of glycoprotein gE reduces the propagation of pseudorabies virus in the nervous system of mice after intranasal inoculation. Virology 219, 279-284.

Barnett, E.M., Evans, G.D., Sun, N.K, Perlman, S., Cassel, M.D., 1995. Anterograde tracing of trigeminal afferent pathways from the murine tooth pulp to cortex using herpes simplex virus type 1. J. Neurosci. 15, 2972–2984.

Bauer, A., Nolden, T., Schröter, J., Römer-Oberdörfer, A., Gluska, S, Perlson, E, Finke, S. 2014. Anterograde glycoprotein-dependent transport of newly generated rabies virus in dorsal root ganglion neurons. J. Virol. 88, 14172-14183.

Beier, K.T. 2019. Hitchhiking on the neuronal highway: mechanisms of transsynaptic specificity. J. Chem. Neuroanat. 99, 9-17.

Beier, K.T., Saunders, A., Oldenburg, I.A., Miyamichi, K., Akhtar, N., Luo, L., Whelan, S.P., Sabatini, B., Cepko, C.L., 2011. Anterograde or retrograde transsynaptic labeling of CNS neurons with vesicular stomatitis virus vectors. Proc. Natl. Acad. Sci. U.S.A. 108, 5414-5419.

Beier, K.T., Saunders, A.B., Oldenburg, I.A., Sabatini, B.L., Cepko, C.L., 2013. Vesicular stomatitis virus with the rabies virus glycoprotein directs retrograde transsynaptic transport among neurons in vivo. Front. Neural Circuits 7, 7:11.

Belot. L., Albertini, A., Gaudin, Y., 2019. Structural and cellular biology of rhabdovirus entry. Adv. Virus Res. 104, 147-183.

Bertoune, M.A.R., Nickl, B., Krieger, T., Wohlers, L., Bonaterra, G.A., Dietzschold, B., Weihe, E., Bette, M., 2017. The phenotype of the RABV glycoprotein determines cellular and global virus load in the brain and is decisive for the pace of the disease. Virology 511, 82-94.

Billig, I., Foris, J.M., Enquist, L.W., Card, J.P., Yates, B.J., 2000. Definition of neuronal circuitry controlling the activity of phrenic and abdominal motoneurons in the ferret using recombinant strains of pseudorabies virus. J. Neurosci. 20, 7446–7454.

Bizzini, B., 1979. Tetanus toxin. Microbiol. Rev. 43, 224–240.

Brideau, A.D., Card, J.P., Enquist, L.W., 2000. Role of pseudorabies virus Us9, a type II membrane protein, in infection of tissue culture cells and the rat nervous system. J. Virol. 74, 834-45.

Bostan, A.C., Dum, R.P., Strick, P.L., 2010. The basal ganglia communicate with the cerebellum. Proc. Natl. Acad. Sci. U.S.A. 107, 8452-8456.

Butowt, R., von Bartheld, C.S., 2003. Connecting the dots: trafficking of neurotrophins, lectins and diverse pathogens by binding to the neurotrophin receptor p75NTR. Eur. J. Neurosci. 17, 673-680.

Büttner-Ennever, J.A., Grob, P., Akert, K., Bizzini, B., 1981. Transsynaptic retrograde labeling in the oculomotor system of the monkey with [125I] tetanus toxin BIIb fragment. Neurosci. Lett. 26, 233-238.

Caillet-Saguy, C., Maisonneuve, P., Delhommel, F., Terrien, E., Babault, N., Lafon, M., Cordier, F., Wolff, N., 2015. Strategies to interfere with PDZ-mediated interactions in neurons: What we can learn from the rabies virus. Prog. Biophys. Mol. Biol. 119, 53-59.

Callaway, E.M., Luo, L., 2015. Monosynaptic Circuit Tracing with Glycoprotein-Deleted Rabies Viruses. J. Neurosci. 35, 8979-8985.

Card, J.P., Enquist, L.W., Moore, R.Y., 1999. Neuroinvasiveness of pseudorabies virus injected intracerebrally is dependent on viral concentration and terminal field density. J. Comp. Neurol. 407, 438-452.

Card. J.P., Whealy, M.E., Robbins, A.K., Enquist, L.W., 1992. Pseudorabies virus envelope glycoprotein gI influences both neurotropism and virulence during infection of the rat visual system. J. Virol. 66, 3032-3041.

Card, J.P., Whealy, M.E., Robbins, A.K., Moore, R.Y., Enquist, L.W., 1991. Two alpha-herpesvirus strains are transported differentially in the rodent visual system. Neuron 6, 957-969.

Campadelli-Fiume, G., Cocchi, F., Menotti, L., Lopez, M., 2000. The novel receptors that mediate the entry of herpes simplex viruses and animal alphaherpesviruses into cells. Rev. Med. Virol. 10, 305-319.

Cano, G., Card, J.P., Sved, A.F., 2004.Dual viral transneuronal tracing of central autonomic circuits involved in the innervation of the two kidneys in the rat. J. Comp. Neurol. 471, 462-481.

Charlton, K.M., Casey, G.A., Wandeler, A.I., Nadin-Davis, S. 1996. Early events in rabies virus infection of the central nervous system in skunks (Mephitis mephitis). Acta Neuropathol. 91, 89-98.

Chen, S., Ming, X., Miselis, R., Aston-Jones, G., 1999. Characterization of transsynaptic tracing with central application of Pseudorabies virus. Brain Res. 838, 171-183.

Ciabatti, E., Gonzalez-Rueda, A., Mariotti, L, Morgese, F., Tripodi, M., 2017. Life-Long Genetic and Functional Access to Neural Circuits Using Self-Inactivating Rabies Virus. Cell 170, 382-392.

Clark, H.F., 1980. Rabies serogroup viruses in neuroblastoma cells: propagation, "autointerference," and apparently random back-mutation of attenuated viruses to the virulent state. Infect. Immun. 27, 1012-1022.

Coffman, K.A., Dum, R.P. Strick, P.L., 2011. Cerebellar vermis is a target of projections from the motor areas in the cerebral cortex. Proc. Natl. Acad. Sci. U.S.A. 108, 16068-16073.

Conzelmann, K.K., Cox, J.H., Schneider, L.G., Thiel, H.J., 1990. Molecular cloning and complete nucleotide sequence of the attenuated rabies virus SAD B19. Virology 175, 485-499.

Conzelmann K.K., 1996. Genetic manipulation of non-segmented negative-strand RNA viruses. J. Gen. Virol. 77, 381-389.

Cornish, T.E., Stallknecht, D.E., Brown, C.C., Seal, B.S., Howerth, E.W., 2001. Pathogenesis of experimental vesicular stomatitis virus (New Jersey serotype) infection in the deer mouse (Peromyscus maniculatus). Vet. Pathol. 38, 396-406.

Coulon, P., Rollin, P.E., Flamand, A., 1983. Molecular basis of rabies virus virulence. II. Identification of a site on the CVS glycoprotein associated with virulence. J. Gen. Virol. 64, 693-696.

Coulon, P., Derbin, C., Kucera, P., Lafay, F., Prehaud, C., Flamand, A., 1989. Invasion of the peripheral nervous systems of adult mice by the CVS strain of rabies virus and its avirulent derivative AvO1. J. Virol. 63, 3550-3554.

Coulon, P., Bras, H., Vinay, L., 2011. Characterization of last-order premotor interneurons by transneuronal tracing with rabies virus in the neonatal mouse spinal cord. J. Comp. Neurol. 519, 3470-3487.

Davis, B.M., Rall, G.F., Schnell, M.J., 2015. Everything You Always Wanted to Know About Rabies Virus (But Were Afraid to Ask). Annu. Rev Virol. 2, 451-471.

Dietzschold, B., Schnell, M., Koprowski, H., 2005. Pathogenesis of rabies. Curr. Top. Microbiol. Immunol. 292, 45-56.

Dietzschold, B., Li, J., Faber, M., Schnell, M., 2008. Concepts in the pathogenesis of rabies. Future Virol. 3, 481-490.

Dietzschold, B., Wiktor, T.J., Trojanowski, J.Q., Macfarlan, R.I., Wunner, W.H., Torres-Anjel, M.J., Koprowski, H., 1985. Differences in cell-to-cell spread of pathogenic and apathogenic rabies virus in vivo and in vitro. J. Virol. 56, 12-18.

Dietzschold, B., Wunner, W.H., Wiktor, T.J., Lopes, A.D., Lafon, M., Smith, C.L., Koprowski, H., 1983. Characterization of an antigenic determinant of the glycoprotein that correlates with pathogenicity of rabies virus. Proc. Natl. Acad. Sci. U.S.A. 80, 70-74.

Dum, R.P., Levinthal, D.J., Strick, P.L., 2016. Motor, cognitive, and affective areas of the cerebral cortex influence the adrenal medulla. Proc. Natl. Acad. Sci. U.S.A. 113, 9922-9927.

Enquist, L.W., Card, J.P., 1996. Pseudorabies virus: a tool for tracing neuronal connections. In: Lowenstein, P.R., Enquist, L.W. (Eds), Protocols for Gene Transfer in Neuroscience: Towards Gene Therapy of Neurological Disorders. John Wiley & Sons, Chichester, pp. 333-358.

Enquist, L.W., Card, J.P., 2003. Recent advances in the use of neurotropic viruses for circuit analysis. Curr. Opin. Neurobiol. 13, 603-606.

Enquist, L.W., Leib, D.A., 2016. Intrinsic and Innate Defenses of Neurons: Détente with the Herpesviruses. J. Virol. 91(1).

Etessami, R., Conzelmann, K.K., Fadai-Ghotbi, B., Natelson, B., Tsiang, H., Ceccaldi, P.E., 2000. Spread and pathogenic characteristics of a G-deficient rabies virus recombinant: an in vitro and in vivo study. J. Gen. Virol. 81, 2147-2153.

Faber, M., Pulmanausahakul, R., Nagao, K., Prosniak, M., Rice, A. B., Koprowski, H., Schnell, M.J., Dietzschold, B., 2004. Identification of viral genomic elements responsible for rabies virus neuroinvasiveness. Proc. Natl. Acad. Sci. U.S.A. 101, 16328-16332.

Faul, E.J., Lyles, D.S., Schnell, M.J., 2009. Interferon response and viral evasion by members of the family rhabdoviridae Viruses 1, 832-851.

Fay, R.A., Norgren, R., 1997. Identification of rat brainstem multisynaptic connections to the oral motor nuclei using pseudorabies virus. III. Lingual muscle motor systems. Brain Res. Rev. 25, 291-311.

Finke, S., Conzelmann, K.K., 2005. Replication strategies of rabies virus. Virus Res. 111, 120-31.

Finkelshtein, D., Werman, A., Novick, D., Barak, S., Rubinstein, M., 2013. LDL receptor and its family members serve as the cellular receptors for vesicular stomatitis virus. Proc. Natl. Acad. Sci. U.S.A. 110, 7306-7311.

Garner, J.A., LaVail, J.H., 1999. Differential anterograde transport of HSV type 1 viral strains in the murine optic pathway. J Neurovirol. 5, 140-150.

Gluska, S., Zahavi, E.E., Chein, M., Gradus, T., Bauer, A., Finke, S., Perlson, E., 2014. Rabies Virus Hijacks and accelerates the p75NTR retrograde axonal transport machinery. PLoS Pathog. 10, e1004348.

Graf, W., Gerrits, N., Yatim-Dhiba, N., Ugolini, G., 2002. Mapping the oculomotor system: the power of transneuronal labeling with rabies virus. Eur. J. Neurosci. 15, 1557-1562.

Grafstein, B., Forman, D.S., 1980. Intracellular transport in neurons. Physiol. Rev. 60, 1167-1283.

Grantyn, A., Brandi, A.M., Dubayle, D., Graf, W., Ugolini, G., Hadjidimitrakis, K., Moschovakis, A., 2002. Density gradients of trans-synaptically labeled collicular neurons after injection of rabies virus in the lateral rectus muscle of the rhesus monkey. J. Comp. Neurol. 451, 346-361.

Guo, Y., Duan, M., Wang, X., Gao, J., Guan, Z., Zhang, M., 2019. Early events in rabies virus infection-Attachment, entry, and intracellular trafficking. Virus Res. 263, 217-225.

Haberl, M.G., Viana da Silva, S., Guest, J.M., Ginger, M., Ghanem, A., Mulle, C., Oberlaender, M., Conzelmann, K.K., Frick, A., 2015. An anterograde rabies virus vector for high-resolution large-scale reconstruction of 3D neuron morphology. Brain Struct. Funct. 220, 1369-1379.

Haberl, M.G., Ginger, M., Frick, A., 2017. Dual Anterograde and Retrograde Viral Tracing of Reciprocal Connectivity. Methods Mol. Biol. 1538, 321-340.

Hanham, C.A., Zhao, F., Tignor, G.H., 1993. Evidence from the anti-idiotypic network that the acetylcholine receptor is a rabies virus receptor. J. Virol. 67, 530-542.

Harrison, P.J., Hultborn, H., Jankowska, E., Katz, R., Storai, B., Zytnicki, D., 1984. Labelling of interneurones by retrograde transsynaptic transport of horseradish peroxidase from motoneurones in rats and cats. Neurosci Lett. 45, 15-19.

Hemachudha, T., Ugolini, G., Wacharapluesadee, S., Sungkarat, W., Shuangshoti, S., Laothamatas, J., 2013. Human Rabies: Neuropathogenesis, Diagnosis and Management. Lancel Neurol. 12, 498-513.

Hoover, J.E., Strick, P.L., 1993. Multiple output channels in the basal ganglia. Science 259, 819-821.

Horn, A.K., Buttner-Ennever, J.A., 1990. The time course of retrograde transsynaptic transport of tetanus toxin fragment C in the oculo-motor system of the rabbit after injection into extraocular eye muscles. Exp. Brain Res. 81, 353-362.

Horn, A.K., Buttner-Ennever, J.A., Suzuki, Y., Henn, V., 1995. Histological identification of premotor neurons for horizontal saccades in monkey and man by parvalbumin immunostaining. J. Comp. Neurol. 359, 350-363.

Hoshi, E., Tremblay, L., Féger, J., Carras, P.L., Strick, P.L., 2005. The cerebellum communicates with the basal ganglia. Nat Neurosci 8, 1491-1493.

Huang, J., Zhang, Y., Huang, Y., Gnanadurai, C.W., Zhou, M., Zhao, L., Fu, Z.F., 2017. The ectodomain of rabies virus glycoprotein determines dendritic cell activation. Antiviral Res. 141, 1-6.

Huneycutt, B.S., Plakhov, I.V., Shusterman, Z., Bartido, S.M., Huang, A., Reiss, C.S., Aoki, C., 1994. Distribution of vesicular stomatitis virus proteins in the brains of BALB/c mice following intranasal inoculation: an immunohistochemical analysis. Brain Res. 635, 81-95.

Jackson, A.C., 1991. Biological basis of rabies virus neurovirulence in mice: comparative pathogenesis study using the immunoperoxidase technique. J. Virol. 65, 537-540.

Jackson, A.C., Park, H., 1999. Experimental rabies virus infection of p75 neurotrophin receptor-deficient mice. Acta Neuropathol. 98, 641-644.

Jacob, Y., Badrane, H., Ceccaldi, P.E., Tordo, N., 2000. Cytoplasmic dynein LC8 interacts with lyssavirus phosphoprotein. J. Virol. 74, 10217-10222.

Jankowska, E., 1985. Further indications for enhancement of retrograde transneuronal transport of WGA-HRP by synaptic activity. Brain Res. 341, 403-408.

Jankowska, E., Skoog, B., 1986. Labelling of midlumbar neurones projecting to cat hindlimb motoneurones by transneuronal transport of a horseradish peroxidase conjugate. Neurosci. Lett. 71, 163-168.

Jansen, A.S., Nguyen, X.V., Karpitskiy, V., Mettenleiter, T.C., Loewy, A.D., 1995. Central command neurons of the sympathetic nervous system: basis of the fight-or-flight response. Science 270, 644-646.

Jespersen, N.E., Leyrat, C., Gérard, F.C., Bourhis, J.M., Blondel, D., Jamin, M., Barbar, E., 2019. The LC8-RavP ensemble Structure Evinces A Role for LC8 in Regulating Lyssavirus Polymerase Functionality. J. Mol Biol. 431, 4959-4977.

Johnson, R.T., 1982. Pathogenesis of CNS infections. In: Johnson, R.T. (Ed.), Viral Infections of the Nervous System. Raven Press, New York, pp. 37-60.

Jwair, S., Coulon, P., Ruigrok, T.J., 2017. Disynaptic Subthalamic Input to the Posterior Cerebellum in Rat. Front. Neuroanat. 11:13.

Kaplan, A.S., 1969. Herpes Simplex and Pseudorabies Virus. Virology Monographs, No. 5, Springer, Vienna.

Kelly, R.M., Strick, P.L., 2000. Rabies as a transneuronal tracer of circuits in the central nervous system. J. Neurosci. Methods 103, 63-71.

Kelly, R.M., Strick, P.L., 2003. Cerebellar loops with motor cortex and prefrontal cortex of a nonhuman primate. J. Neurosci. 23, 8432-8444.

Kim, E.J., Jacobs, M.W., Ito-Cole, T., Callaway, E.M., 2016. Improved Monosynaptic Neural Circuit Tracing Using Engineered Rabies Virus Glycoproteins. Cell Rep. 15, 692-699.

Klingen, Y., Conzelmann, K.K., Finke, S., 2008. Double-labeled rabies virus: live tracking of enveloped virus transport. J. Virol. 82, 237-245.

Kottke, T., Errington, F., Pulido, J., Galivo, F., Thompson, J., Wongthida, P., Diaz, R.M., Chong, H., Ilett, E., Chester, J., Pandha, H., Harrington, K., Selby, P., Melcher, A., Vile, R., 2011. Broad antigenic coverage induced by vaccination with virus-based cDNA libraries cures established tumors. Nat. Med. 17, 854-859.

Kramer, T., Enquist, L.W., 2013. Directional spread of alphaherpesviruses in the nervous system. Viruses. 5, 678-707.

Kristensson, K., Ghetti, B., Wiśniewski, H.M., 1974. Study on the propagation of Herpes simplex virus (type 2) into the brain after intraocular injection. Brain Res. 69, 189-201.

Kuypers, H.G.J.M., Ugolini, G., 1990. Viruses as transneuronal tracers. Trends Neurosci. 13, 71–75.

Lafay, F., Coulon, P., Astic, L., Saucier, D., Riche, D., Holley, A., Flamand, A., 1991. Spread of the CVS strain of rabies virus and of the avirulent mutant AvO1 along the olfactory pathways of the mouse after intranasal inoculation. Virology 183, 320-330.

Lafon, M., 2005. Rabies virus receptors. J. Neurovirol. 11, 82-87.

Lafon, M., 2008. Immune evasion, a critical strategy for rabies virus. Dev Biol (Basel) 131, 413-419.

Lafon, M., Bourhy, H., Sureau, P., 1988. Immunity against the European bat rabies (Duvenhage) virus induced by rabies vaccines: an experimental study in mice. Vaccine 6, 362-368.

Lentz, T.L., Burrage, T.G., Smith, A.L., Crick, J., Tignor, G.H., 1982. Is the acetylcholine receptor a rabies virus receptor? Science 215, 182-184.

Levinthal, D.J., Strick, P.L., 2012. The motor cortex communicates with the kidney. J. Neurosci. 32, 6726-6731.

Lin, K., Zhong, X., Ying, M., Li, L., Tao, S., Zhu, X., He, X., Xu, F., 2020. A mutant vesicular stomatitis virus with reduced cytotoxicity and enhanced anterograde trans-synaptic efficiency. Mol. Brain 13, 45.

Lo, L., Anderson, D.J., 2011. A Cre-dependent, anterograde transsynaptic viral tracer for mapping output pathways of genetically marked neurons. Neuron 72, 938-950.

Loewy, A.D., 1995. Pseudorabies virus: a transneuronal tracer for neuroanatomical studies. In: Keplitt, M., Loewy, AD. (Eds), Viral Vectors: Gene Therapy and Neuroscience Applications. Academic Press, New York, pp. 349-366.

López., I.P., Salin, P., Kachidian, P., Barroso-Chinea, P., Rico, A.J., Gómez-Bautista, V., Conte-Perales, L., Coulon, P., Kerkerian-Le Goff, L., Lanciego, J.L., 2010. The added value of rabies virus as a retrograde tracer when combined with dual anterograde tract-tracing. J. Neurosci. Methods. 194, 21-27.

Lundh, B., 1990. Spread of vesicular stomatitis virus along the visual pathways after retinal infection in the mouse. Acta Neuropathol. 79, 395-401.

Lundh, B., Kristensson, K., Norrby, E., 1987. Selective infections of olfactory and respiratory epithelium by vesicular stomatitis and Sendai viruses. Neuropathol. Appl. Neurobiol. 13, 111-122.

Lundh, B., Löve, A., Kristensson, K., Norrby, E., 1988. Non-lethal infection of aminergic reticular core neurons: age-dependent spread of ts mutant vesicular stomatitis virus from the nose. J. Neuropathol. Exp. Neurol. 47, 497-506.

Lycke, E., Tsiang, H., 1987. Rabies virus infection of cultured rat sensory neurons. J. Virol. 61, 2733-2741.

Lycke, E., Kristensson, K., Svennerholm, B., Vahlne, A., Ziegler, R., 1984. Uptake and transport of herpes simplex virus in neurites of rat dorsal root ganglia cells in culture. J. Gen. Virol. 65, 55-64.

MacGibeny, M.A., Koyuncu, O.O., Wirblich, C., Schnell, M.J., Enquist, L.W., 2018. Retrograde axonal transport of rabies virus is unaffected by interferon treatment but blocked by emetine locally in axons. PLoS Pathog. 14, e1007188.

Maday, S., Twelvetrees, A.E., Moughamian, A.J., Holzbaur, E.L., 2014. Axonal transport: cargo-specific mechanisms of motility and regulation. Neuron 84, 292-309.

Marson. L., McKenna, K.E., 1996. CNS cell groups involved in the control of the ischiocavernosus and bulbospongiosus muscles: a transneuronal tracing study using pseudorabies virus. J. Comp. Neurol. 374, 161-79.

May, P.J., Warren, S., Gamlin, P.D.R., Billig, I., 2018. An Anatomic Characterization of the Midbrain Near Response Neurons in the Macaque Monkey. Invest. Ophthalmol. Vis. Sci. 59, 1486-1502.

Mazarakis, N.D., Azzouz, M., Rohll, J.B., Ellard, F.M., Wilkes, F.J., Olsen, A.L., Carter, E.E., Barber, R.D., Baban, D.F., Kingsman, S.M., Kingsman, A.J., O'Malley, K., Mitrophanous, K.A., 2001. Rabies virus

glycoprotein pseudotyping of lentiviral vectors enables retrograde axonal transport and access to the nervous system after peripheral delivery. Hum. Mol. Genet. 10, 2109-2121.

McGovern, A.E., Davis-Poynter, N., Rakoczy, J., Phipps, S., Simmons, D.G., Mazzone, S.B., 2012. Anterograde neuronal circuit tracing using a genetically modified herpes simplex virus expressing EGFP. J. Neurosci. Methods 209, 158-167.

Mebatsion, T., 2001. Extensive attenuation of rabies virus by simultaneously modifying the dynein light chain binding site in the P protein and replacing Arg333 in the G protein. J. Virol. 75, 11496-11502.

Mebatsion, T., Konig, M., Conzelmann, K.K., 1996a. Budding of rabies virus particles in the absence of the spike glycoprotein. Cell 84, 941-951.

Mebatsion, T., Schnell, M.J., Cox, J.H., Finke, S., Conzelmann, K.K., 1996b. Highly stable expression of a foreign gene from rabies virus vectors. Proc. Natl. Acad. Sci. U.S.A. 93, 7310-7314.

Mebatsion, T., Weiland, F., Conzelmann, K.K., 1999. Matrix protein of rabies virus is responsible for the assembly and budding of bullet-shaped particles and interacts with the transmembrane spike glycoprotein G. J. Virol. 73, 242-250.

Melzer, M.K., Lopez-Martinez, A., Altomonte, J., 2017. Oncolytic Vesicular Stomatitis Virus as a Viro-Immunotherapy: Defeating Cancer with a "Hammer" and "Anvil". Biomedicines. 5(1).

Mettenleiter, T.C., 2003. Pathogenesis of neurotropic herpesviruses: role of viral glycoproteins in neuroinvasion and transneuronal spread. Virus Res. 92, 197-206.

Miñana, R., Duran, J.M., Tomas, M., Renau-Piqueras, J., Guerri, C., 2001. Neural cell adhesion molecule is endocytosed via a clathrin-dependent pathway. Eur. J. Neurosci. 13, 749-756.

Miyachi, S., Lu, X., Imanishi, M., Sawada, K., Nambu, A., Takada, M., 2006. Somatotopically arranged inputs from putamen and subthalamic nucleus to primary motor cortex. Neurosci Res 56, 300-308.

Morcuende, S., Delgado-García, J.M., Ugolini, G., 2002. Neuronal premotor networks involved in eyelid responses: retrograde transneuronal tracing with rabies virus from the orbicularis oculi muscle in the rat. J. Neurosci. 22, 8808-8818.

Morecraft, R.J., Ugolini, G., Lanciego, J.L., Wouterlood, F.G., Pandya, D.N., 2014. Classic and Contemporary neural tract tracing techniques. In: Johansen−Berg H., Behrens, T. (Eds.), Diffusion MRI, 2nd Edition: From Quantitative Measurement to In−Vivo Neuroanatomy. London, Academic Press, Elsevier, Amsterdam, Chapter 17, pp. 359-399.

Morimoto, K., Patel, M., Corisdeo, S., Hooper, D.C., Fu, Z.F., Rupprecht, C.E., Koprowski, H., Dietzschold, B. 1996. Characterization of a unique variant of bat rabies virus responsible for newly emerging human cases in North America. Proc. Natl. Acad. Sci. U.S.A. 93, 5653-5658.

Morimoto, K., Hooper, D.C., Carbaugh, H., Fu, Z.F., Koprowski, H., Dietzschold, B., 1998. Rabies virus quasispecies: implications for pathogenesis. Proc. Natl. Acad. Sci. U.S.A. 95, 3152-3156.

Morimoto, K., Hooper, D.C., Spitsin, S., Koprowski, H., Dietzschold, B., 1999. Pathogenicity of different rabies virus variants inversely correlates with apoptosis and rabies virus glycoprotein expression in infected primary neuron cultures. J. Virol. 73, 510-518.

Moschovakis, A.K., Gregoriou, G.G., Ugolini, G., Doldan, M., Graf, W., Guldin, W., Hadjidimitrakis, K., Savaki, H.E., 2004. Oculomotor areas of the primate frontal lobes: a transneuronal transfer of rabies virus and [14C]-2-deoxyglucose functional imaging study. J. Neurosci. 24, 5726-5740.

Murphy, F.A., Bauer, S.P. 1974. Early street rabies virus infection in striated muscle and later progression to the central nervous system. Intervirology 3, 256-268.

Murphy, F.A., Bauer, S.P., Harrison, A.K., Winn, W.C. Jr. 1973a. Comparative pathogenesis of rabies and rabies-like viruses. Viral infection and transit from inoculation site to the central nervous system. Lab. Invest. 28, 361-376.

Murphy, F.A., Harrison, A.K., Winn, W.C., Bauer, S.P. 1973b Comparative pathogenesis of rabies and rabies-like viruses: infection of the central nervous system and centrifugal spread of virus to peripheral tissues. Lab. Invest. 29, 1-16.

Nabb, A.T., Frank, M., Bentley, M., 2020. Smart motors and cargo steering drive kinesin-mediated selective transport. Mol. Cell. Neurosci. 103, 103464. doi: 10.1016/j.mcn.2019.103464. [Epub ahead of print]

Oksayan, S., Ito, N., Moseley, G., Blondel, D., 2012. Subcellular trafficking in rhabdovirus infection and immune evasion: a novel target for therapeutics. Infect. Disord. Drug Targets 12, 38-58.

Ohara, S,. Inoue, K., Yamada, M., Yamawaki, T., Koganezawa, N., Tsutsui, K., Witter, M.P., Iijima, T., 2009a. Dual transneuronal tracing in the rat entorhinal-hippocampal circuit by intracerebral injection of recombinant rabies virus vectors. Front. Neuroanat. 3:1.

Ohara, S., Inoue, K., Witter, M.P., Iijima, T., 2009b. Untangling neural networks with dual retrograde transsynaptic viral infection. Front Neurosci. 3, 344-349.

Ohara, S., Sato, S., Tsutsui, K., Witter, M.P., Iijima, T., 2013a. Organization of multisynaptic inputs to the dorsal and ventral dentate gyrus: retrograde trans-synaptic tracing with rabies virus vector in the rat. PLoS One 8, e78928.

Ohara, S., Sato, S., Oyama, K., Tsutsui, K., Iijima, T., 2013b. Rabies virus vector transgene expression level and cytotoxicity improvement induced by deletion of glycoprotein gene. PLoS One 8, e80245.

Ohara, S., Sota, Y., Sato, S., Tsutsui, K.I., Iijima, T., 2017. Increased transgene expression level of rabies virus vector for transsynaptic tracing. PLoS One. 12, e0180960.

Osakada, F., Mori, T., Cetin, A.H., Marshel, J.H., Virgen, B., Callaway, E.M., 2011. New rabies virus variants for monitoring and manipulating activity and gene expression in defined neural circuits. Neuron 71, 617-631.

Perreault, M.C., Bernier, A.P., Renaud, J.S., Roux, S., Glover, J.C., 2006. C fragment of tetanus toxin hybrid proteins evaluated for muscle-specific transsynaptic mapping of spinal motor circuitry in the newborn mouse. Neuroscience 141, 803-816.

Piccinotti, S., Whelan, S.P., 2016. Rabies Internalizes into Primary Peripheral Neurons via Clathrin Coated Pits and Requires Fusion at the Cell Body. PLoS Pathog. 12, e1005753.

Plakhov, I.V., Arlund, E.E., Aoki, C., Reiss, C.S., 1995. The earliest events in vesicular stomatitis virus infection of the murine olfactory neuroepithelium and entry of the central nervous system. Virology 209, 257-262.

Poisson, N., Real, E., Gaudin, Y., Vaney, M.C., King, S., Jacob, Y., Tordo, N., Blondel, D., 2001. Molecular basis for the interaction between rabies virus phosphoprotein P and the dynein light chain LC8: dissociation of dynein-binding properties and transcriptional functionality of P. J. Gen. Virol. 82, 2691-2696.

Porter, J.D., Guthrie, B.L., Sparks, D.L., 1985. Selective retrograde transneuronal transport of wheat germ agglutinin-conjugated horseradish peroxidase in the oculomotor system. Exp. Brain Res. 57, 411-416.

Préhaud, C., Wolff, N., Terrien, E., Lafage, M., Mégret, F., Babault, N., Cordier, F., Tan, G.S., Maitrepierre, E., Ménager, P., Chopy, D., Hoos, S., England, P., Delepierre, M., Schnell, M.J., Buc, H., Lafon, M., 2010. Attenuation of rabies virulence: takeover by the cytoplasmic domain of its envelope protein. Sci. Signal 3(105):ra5.

Prevosto, V., Graf, W., Ugolini, G., 2009. Posterior parietal cortex areas MIP and LIPv receive eye position and velocity inputs via ascending preposito-thalamo-cortical pathways. Eur. J. Neurosci. 30, 1151-1161.

Prevosto, V., Graf, W., Ugolini, G., 2010. Cerebellar inputs to intraparietal cortex areas LIP and MIP: functional frameworks for adaptive control of eye movements, reaching and arm/eye/head movement coordination. Cereb. Cortex 20, 214-228.

Prevosto, V., Graf, W., Ugolini, G., 2011. Proprioceptive pathways to posterior parietal areas MIP and LIPv from the dorsal column nuclei and the postcentral somatosensory cortex. Eur. J. Neurosci. 33, 444-460.

Prevosto, V., Graf, W., Ugolini, G., 2017. The control of eye movements by the cerebellar nuclei: polysynaptic projections from the fastigial, interpositus posterior and dentate nuclei to lateral rectus motoneurons in primates. Eur. J. Neurosci. 45, 1538-1552.

Rathelot, J.A., Strick, P.L., 2006. Muscle representation in the macaque motor cortex: an anatomical perspective. Proc. Nat. Acad. Sci. U.S.A. 103, 8257-8262.

Rathelot, J.A., Strick, P.L., 2009. Subdivisions of primary motor cortex based on cortico-motoneuronal cells. Proc. Nat. Acad. Sci. U.S.A. 106, 918-923.

Raux, H., Flamand, A., Blondel, D., 2000. Interaction of the rabies virus P protein with the LC8 dynein light chain. J. Virol. 74, 10212-10216.

Reardon, T.R., Murray, A.J., Turi, G.F., Wirblich, C., Croce, K.R., Schnell, M.J., Jessell, T.M., Losonczy, A., 2016. Rabies Virus CVS-N2c(ΔG) Strain Enhances Retrograde Synaptic Transfer and Neuronal Viability. Neuron 89, 711-724.

Rice, C.D., Lois, J.H., Kerman, I.A., Yates, B.J., 2009. Localization of serotoninergic neurons that participate in regulating diaphragm activity in the cat. Brain Res. 1279, 71-81.

Rice, C.D., Weber, S.A., Waggoner, A.L., Jessell, M.E., Yates, B.J., 2010. Mapping of neural pathways that influence diaphragm activity and project to the lumbar spinal cord in cats. Exp Brain Res. 203, 205-211.

Rieder, M., Conzelmann, K.K., 2009. Rhabdovirus evasion of the interferon system. J. Interferon Cytokine Res. 29, 499-509.

Rinaman, L., Card, J.P., Enquist, L.W., 1993. Spatiotemporal responses of astrocytes, ramified microglia, and brain macrophages to central neuronal infection with pseudorabies virus. J. Neurosci. 13, 685-702.

Roizman, B., 1996. Herpesviridae. In: Fields, B.N., Knipe, D.M., Howley, P.M. (Eds), Field's virology, 3rd edition. Lippincott–Raven Publishers, Philadelphia, pp. 2221-2230.

Rotto-Percelay, D.M., Wheeler, J.G., Osorio, F.A., Platt, K.B., Loewy, A.D., 1992. Transneuronal labeling of spinal interneurons and sympathetic preganglionic neurons after pseudorabies virus injections in the rat medial gastrocnemius muscle. Brain Res. 574, 291-306.

Rudolf, R., Straka, T., 2019. Nicotinic acetylcholine receptor at vertebrate motor endplates: Endocytosis, recycling, and degradation. Neurosci Lett. 711, 134434.

Ruskell, G.L., 1973. Sympathetic innervation of the ciliary muscle in monkeys. Exp. Eye Res. 16, 183-190.

Sacramento, D., Badrane, H., Bourhy, H., Tordo, N., 1992. Molecular epidemiology of rabies virus in France: comparison with vaccine strains. J. Gen. Virol. 73, 1149-1158.

Salin, P., Castle, M., Kachidian, P., Barroso-Chinea, P., López, I.P., Rico, A.J., Kerkerian-Le Goff, L., Coulon, P., Lanciego, J.L., 2008. High-resolution neuroanatomical tract-tracing for the analysis of striatal microcircuits. Brain Res. 1221, 49-58.

Salin, P., López, I.P., Kachidian, P., Barroso-Chinea, P., Rico, A.J., Gómez-Bautista, V., Coulon, P., Kerkerian-Le Goff, L., Lanciego, J.L., 2009. Changes to interneuron-driven striatal microcircuits in a rat model of Parkinson's disease. Neurobiol. Dis. 34, 545-552.

Sawchenko, P.E., Gerfen, C.E., 1985. Plant lectins and bacterial toxins as tools for tracing neuronal connections. Trends Neurosci. 8, 378-384.

Schell, J.B., Rose, N.F., Bahl, K., Diller, K., Buonocore, L., Hunter, M., Marx, P.A., Gambhira, R., Tang, H., Montefiori, D.C., Johnson, W.E., Rose, J.K., 2011. Significant protection against high-dose simian immunodeficiency virus challenge conferred by a new prime-boost vaccine regimen. J. Virol. 85, 5764-5772.

Schnell, M.J., Mebatsion, T., Conzelmann, K.K., 1994. Infectious rabies viruses from cloned cDNA. EMBO J. 13, 4195-4203.

Schnell, M.J., McGettigan, J.P., Wirblich, C., Papaneri, A., 2010. The cell biology of rabies virus: using stealth to reach the brain. Nat. Rev. Microbiol. 8, 51-61.

Seif, I., Coulon, P., Rollin, P.E., Flamand, A., 1985. Rabies virulence: effect on pathogenicity and sequence characterization of rabies virus mutations affecting antigenic site III of the glycoprotein. J. Virol. 53, 926-934.

Smith, J.S., Yager, P.A., Baer, G.M., 1973. A rapid reproducible test for determining rabies neutralizing antibody. Bull. World Health Organ. 48, 535-541.

Smith, J.S., Orciari, L.A., Yager, P.A., Seidel, H.D., Warner, C.K., 1992. Epidemiologic and historical relationships among 87 rabies virus isolates as determined by limited sequence analysis. J. Infect. Dis. 166, 296-307.

Standish, A., Enquist, L.W., Schwaber, J.S., 1994. Innervation of the heart and its central medullary origin defined by viral tracing. Science 263, 232-234.

Stepien, A.E., Tripodi, M., Arber, S., 2010. Monosynaptic rabies virus reveals premotor network organization and synaptic specificity of cholinergic partition cells. Neuron. 68, 456-472.

Strack, A.M., Loewy, A.D., 1990. Pseudorabies virus: a highly specific transneuronal cell body marker in the sympathetic nervous system. J. Neurosci., 10, 2139-2147.

Strack, A.M., Sawyer, W.B., Hughes, J.H., Platt, K.B., Loewy, A.D., 1989a. A general pattern of CNS innervation of the sympathetic outflow demonstrated by transneuronal pseudorabies viral infections. Brain Res. 491, 156-162.

Strack, A.M., Sawyer, W.B., Platt, K.B., Loewy, A.D., 1989b. CNS cell groups regulating the sympathetic outflow to adrenal gland as revealed by transneuronal cell body labeling with pseudorabies virus. Brain Res. 491, 274-296.

Sun, N., Cassell, M.D., Perlman, S., 1996. Anterograde, transneuronal transport of herpes simplex virus type 1 strain H129 in the murine visual system. J. Virol. 70, 5405-5413.

Suzuki, L., Coulon, P., Sabel-Goedknegt, E.H., Ruigrok, T.J., 2012. Organization of cerebral projections to identified cerebellar zones in the posterior cerebellum of the rat. J. Neurosci. 32, 10854-10869.

Szpara, M.L., Parsons, L., Enquist, L.W., 2010. Sequence variability in clinical and laboratory isolates of herpes simplex virus 1 reveals new mutations. J. Virol. 84, 5303-5313.

Tan, G.S., Preuss, M.A., Williams, J.C., Schnell, M.J., 2007. The dynein light chain 8 binding motif of rabies virus phosphoprotein promotes efficient viral transcription. Proc. Natl. Acad. Sci. U.S.A. 104, 7229-7234.

Tang, Y., Rampin, O., Giuliano, F., Ugolini, G., 1999. Spinal and brain circuits to motoneurons of the bulbospongiosus muscle: retrograde transneuronal tracing with rabies virus. J. Comp. Neurol. 414, 167-192.

Thiele, C.J., 1998. Neuroblastoma: In: Masters, J. (Ed.), Human Cell Culture. Kluwer Academic Publishers, Lancaster, UK, Vol 1, pp. 21-53.

Thoulouze, M.I., Lafage, M., Schachner, M., Hartmann, U., Cremer, H., Lafon, M., 1998. The neural cell adhesion molecule is a receptor for rabies virus. J. Virol. 72, 7181-7190.

Tripodi, M., Stepien, A.E., Arber, S., 2011. Motor antagonism exposed by spatial segregation and timing of neurogenesis. Nature 479, 61-66.

Tsiang, H., 1979. Evidence for an intraaxonal transport of fixed and street rabies virus. J. Neuropathol. Exp. Neurol. 38, 286-299.

Tsiang, H., Ceccaldi, P. E., Lycke, E., 1991. Rabies virus infection and transport in human sensory dorsal root ganglia neurons. J. Gen. Virol. 72, 1191-1194.

Tuffereau, C., Bénéjean, J., Blondel, D., Kieffer, B., Flamand, A., 1998. Low-affinity nerve-growth factor receptor (P75NTR) can serve as a receptor for rabies virus. EMBO J. 17, 7250-7259.

Tuffereau, C., Schmidt, K., Langevin, C., Lafay, F., Dechant, G., Koltzenburg, M., 2007. The rabies virus glycoprotein receptor p75NTR is not essential for rabies virus infection. J. Virol. 81, 13622-13630.

Ugolini, G., 1992. Transneuronal transfer of Herpes Simplex virus type 1 (HSV 1) from mixed limb nerves to the CNS. I. Sequence of transfer from sensory, motor and sympathetic nerve fibres to the spinal cord. J. Comp. Neurol 326, 527-548.

Ugolini, G., 1995a**.** Transneuronal tracing with alpha-herpesviruses: a review of the methodology. In: Keplitt M, Loewy AD (Eds), Viral Vectors: Gene Therapy and Neuroscience Applications. Academic Press, New York, pp. 293-317.

Ugolini, G., 1995b. Specificity of rabies virus as a transneuronal tracer of motor networks: transfer from hypoglossal motoneurones to connected second order and higher order central nervous system cell groups. J. Comp. Neurol. 356, 457-480.

Ugolini, G., 1996. Tracing connected neurons with Herpes Simplex Virus type 1. In: Lowenstein, P.R., Enquist, L.W. (Eds.), Protocols for Gene Transfer in Neuroscience: towards Gene Therapy of Neurological Disorders. John Wiley & Sons, Chichester, pp. 349-364.

Ugolini, G., 2008. Use of rabies virus as a transneuronal tracer of neuronal connections: implications for the understanding of rabies pathogenesis. Dev. Biol. (Basel), 131, 493-506.

Ugolini, G., 2010. Advances in viral transneuronal tracing. J. Neurosci. Methods 194, 2-20.

Ugolini, G., 2011. Rabies virus as a transneuronal tracer of neuronal connections. Adv. Virus Res. 79, 165-202.

Ugolini, G., Hemachudha, T., 2018. Rabies: changing prophylaxis and new insights in pathophysiology. Curr. Opin. Infect. Dis. 31, 93-101.

Ugolini, G., Kuypers, H.G.J.M., Simmons, A., 1987. Retrograde transneuronal transfer of Herpes Simplex Virus type 1 (HSV 1) from motoneurones. Brain Res. 422, 242-256.

Ugolini, G., Kuypers, H.G.J.M., Strick, P.L., 1989. Transneuronal transfer of Herpes Virus from peripheral nerves to cortex and brainstem. Science 243, 89-91.

Ugolini, G., Klam, F., Doldan Dans, M., Dubayle, D., Brandi, A.M., Büttner-Ennever, J., Graf, W., 2006. Horizontal eye movement networks in primates as revealed by retrograde transneuronal transfer of rabies virus: differences in monosynaptic input to 'slow' and 'fast' abducens motoneurons. J. Comp. Neurol. 498, 762-785.

Ugolini G., Prevosto V., Graf, W., 2019. Ascending vestibular pathways to parietal areas MIP and LIPv and efference copy inputs from the medial reticular formation: functional frameworks for body representations updating and online movement guidance. Eur. J. Neurosci. 50, 2988-3013.

van den Pol, A.N., Ozduman, K., Wollmann, G., Ho, W.S., Simon, I., Yao, Y., Rose, J.K., Ghosh, P., 2009. Viral strategies for studying the brain, including a replication-restricted self-amplifying delta-G vesicular stomatis virus that rapidly expresses transgenes in brain and can generate a multicolor golgi-like expression. J. Comp. Neurol. 516, 456-481.

Whealy, M.E., Card, J.P., Robbins, A.K., Dubin, J.R., Rziha, H.J., Enquist, L.W., 1993. Specific pseudorabies virus infection of the rat visual system requires both gI and gp63 glycoproteins. J. Virol. 67, 3786-3797.

Wickersham, I.R., Finke, S., Conzelmann, K.K., Callaway, E.M., 2007a. Retrograde neuronal tracing with a deletion-mutant rabies virus. Nat. Methods 4, 47-49.

Wickersham, I.R., Lyon, D.C., Barnard, R.J., Mori, T., Finke, S., Conzelmann, K.K., Young, J.A., Callaway, E.M., 2007b. Monosynaptic restriction of transsynaptic tracing from single, genetically targeted neurons. Neuron 53, 639-647.

Wiesel, T.N., Hubel, D.H., Lam, D.M., 1974. Autoradiographic demonstration of ocular-dominance columns in the monkey striate cortex by means of transneuronal transport. Brain Res. 79, 273-279.

Wirblich, C., Schnell, M.J., 2011. Rabies virus (RV) glycoprotein expression levels are not critical for pathogenicity of RV. J. Virol. 85, 697-704.

Wojaczynski, G.J., Engel, E.A., Steren, K.E., Enquist, L.W., Card, P.J., 2015. The neuroinvasive profiles of H129 (herpes simplex virus type 1) recombinants with putative anterograde-only transneuronal spread properties. Brain Struct. Funct. 220, 1395-1420.

Wunner, W.H., Dietzschold, B., 1987. Rabies virus infection: genetic mutations and the impact on viral pathogenicity and immunity. Contrib. Microbiol. Immunol. 8, 103-124.

Yelverton, E., Norton, S., Obijeski, J.F., Goeddel, D.V., 1983. Rabies virus glycoprotein analogs: biosynthesis in Escherichia coli. Science 219, 614-620.

Zampieri, N., Jessell, T.M., Murray, A.J., 2014. Mapping sensory circuits by anterograde transsynaptic transfer of recombinant rabies virus Neuron. 81, 766-778.

Zemanick, M.C., Strick, P.L., Dix, R.D., 1991. Direction of transneuronal transport of herpes simplex virus 1 in the primate motor system is strain-dependent. Proc. Natl. Acad. Sci. U.S.A. 88, 8048-8051.

Legends

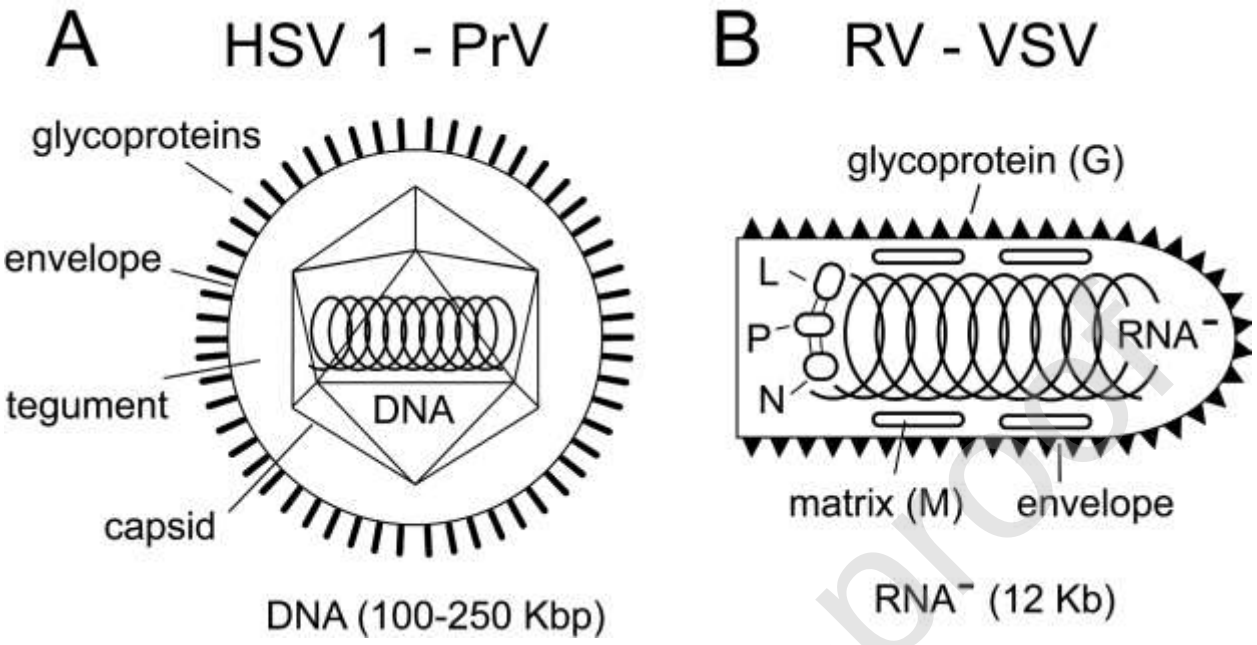

Fig. 1. Virion structure of alpha-herpesviruses (herpes simplex virus type 1, HSV 1, and pseudorabies, PrV) (A) and Rhabdoviruses (Rabies virus, RABV, and vesicular stomatitis virus, VSV) (B). Modified with permission from "Ugolini, G., 2010, Advances in viral transneuronal tracing. J. Neurosci. Methods 194, 2-20". **(A)** Alpha-herpesviruses: the genome (linear double-stranded DNA, 100–250 kbp, encoding more than 30 proteins) is enclosed in an icosahedral capsid, overlaid by a tegument and surrounded by a lipid envelope, on which are anchored more than a dozen glycoproteins types. **(B)** Rhabdoviruses: the virion comprises a central core, containing single-strand, negative sense RNA (12 kb) encapsidated with the nucleoprotein (N), an RNA polymerase (L), and a polymerase cofactor phosphorylated protein (P). The inner core is associated with the matrix protein (M) and is surrounded by a lipid envelope, on which is anchored the glycoprotein (G), which protrudes in trimeric spikes and mediates binding to cellular receptors.

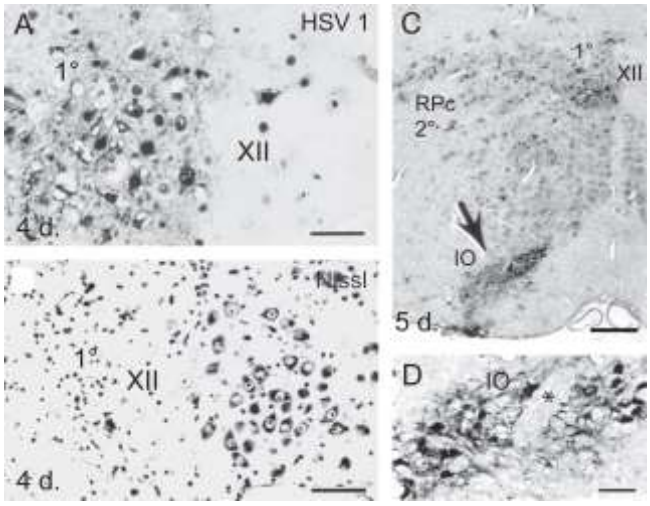

Fig. 2. Retrograde transneuronal transfer of Herpes Simplex Virus type 1 (HSV 1) from the hypoglossal (XII) nerve. Adapted with permission from "Ugolini G., Kuypers, H.G.J.M., Simmons, A., 1987. Retrograde transneuronal transfer of Herpes Simplex Virus type 1 (HSV 1) from motoneurones. Brain Res. 422, 242-256". **(A**) and **(B)** HSV 1 immunolabeling (A) and cresyl violet counterstaining (B) of neighboring sections of the XII nucleus at 4 days: note extensive cell lysis of infected motoneurons (first-order, 1°, A) and loss of Nissl staining (B, cresyl violet) in the left XII nucleus. **(C)** HSV 1 immunolabeling at 5 days: XII nucleus (1°) and retrograde transneuronal labeling in nucleus reticularis parvocellularis (RPc, second-order, 2°) is accompanied by spurious labeling of the inferior olive (IO)(arrow), due to local spread from XII axons. **(D)** High power view of spurious labeling of the IO. Asterisk: XII rootlets crossing the IO. Bars: A,B: 80 µm; C: 250 µm; D: 50 µm.

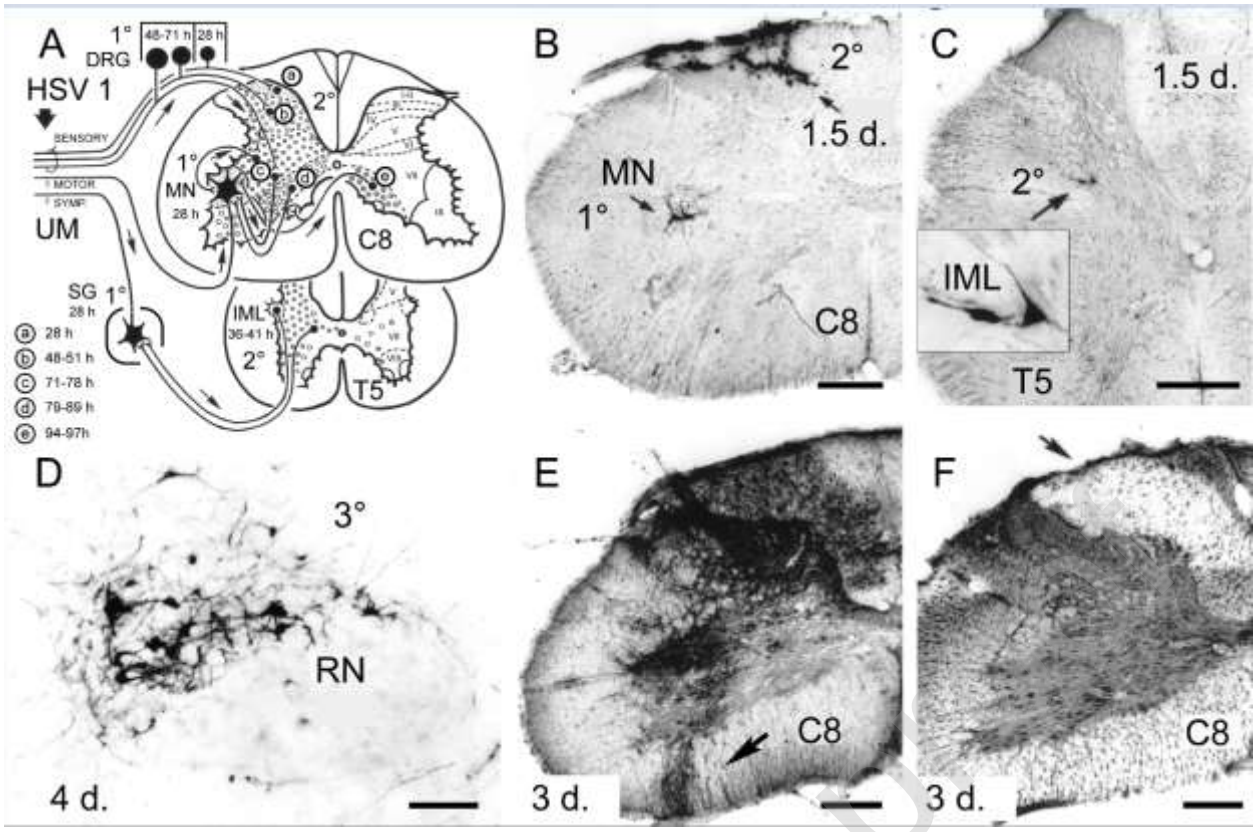

Fig. 3. Transneuronal transfer of Herpes Simplex Virus type 1 (HSV 1) from mixed limb nerves (ulnar and median, UM) to the spinal cord in rats. Adapted with permission from "Ugolini, G., 1992. Transneuronal transfer of Herpes Simplex virus type 1 (HSV 1) from mixed limb nerves to the CNS. I. Sequence of transfer from sensory, motor and sympathetic nerve fibres to the spinal cord. J. Comp. Neurol 326, 527-548". **(A)** Summary of the kinetics of transfer. Anterograde transneuronal transfer from small (nociceptive) primary sensory afferents to the dorsal horn (2°, a) is obtained at short time points (less than 1.5 days), in synchrony with retrograde transneuronal transfer in autonomic pathways (from the stellate ganglion, SG, 1°, to the intermediolateral cell group; IML, 2°). Anterograde transneuronal transfer from primary sensory afferents of larger caliber, as well as retrograde transneuronal transfer from motoneurons (MN) to the spinal intermediate zone (b, c, d, e) require longer time points. DRG: dorsal root ganglia. Roman numerals: spinal laminae. **(B)** HSV 1 immunolabeling in spinal segment C8 at 1.5 days, showing retrogradely labeled MN (1°) and anterograde

transneuronal labeling in superficial sensory laminae of the dorsal horn (2°) and in the dorsal funiculus (glial cells surrounding infected sensory fibers). **(C)** T5 segment at 1.5 days, showing retrograde transneuronal labeling of sympathetic preganglionic neurons (IML, 2°, enlarged in the inset). **(D)** Examples of retrograde transneuronal labeling of supraspinal pathways at 4 days after injection into the UM nerves in rats: contralateral red nucleus (RN) (third-order, 3°) (Ugolini et al., 1989). **(E)** and **(F)** HSV 1 immunolabeling (E) and cresyl violet counterstaining (F) of neighboring sections at C8 at 3 days. Note the loss of Nissl staining of infected glial cells around sensory afferents in the dorsal funiculus (F), and spurious labeling around the axons of retrogradely infected MN within the ventral roots (arrow in E). HSV 1 detection: immunoperoxidase. Bars = B, C, E, F: 300 µm; D: 200 µm.

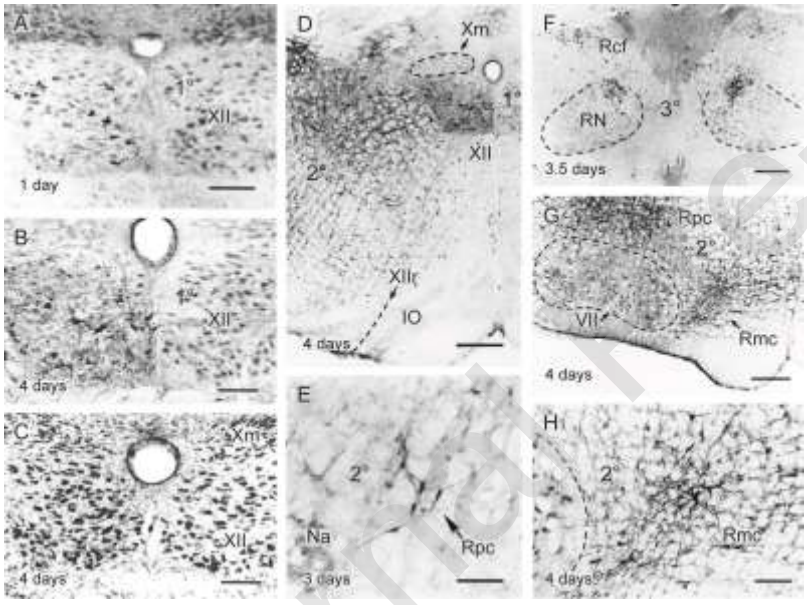

Fig. 4. Retrograde transneuronal transfer of rabies virus (RABV) strain CVS-11 (FR) from the hypoglossal (XII) nerve. Adapted with permission from "Ugolini, G. 1995b. Specificity of rabies virus as a transneuronal tracer of motor networks: transfer from hypoglossal motoneurones to connected second order and higher order central nervous system cell groups. J. Comp. Neurol. 356, 457-480". **(A-C)** Kinetics of infection of XII motoneurons (first-order, 1°): at 1 day, labeling is restricted to cell bodies and proximal dendrites (A), extending to distal

dendrites from 2 days onwards. Even at 4 days, infected motoneurons display normal size and morphology (B) and normal Nissl staining (C, cresyl violet). **(D)** RABV immunolabeling at the level of the XII nucleus at 4 days, showing labeled XII motoneurons (1°) and retrograde transneuronal labeling in the nucleus reticularis parvocellularis (RPc, second-order, 2°, infected from 2.5 days onwards). Even after long-standing infection, there is no spurious labeling of the inferior olive (IO) with RABV, unlike HSV 1 (Fig. 2). **(E)** RABV immunolabeling in RPc (2°) near the nucleus ambiguous (Na) at 3 days. **(F)** Transneuronally labeled third-order neurons (3°) bilaterally in the red nucleus (RN) (dorsal portion) at 3.5 days. **(G)** and **(H)** Section at the level of the facial (VII) nucleus at 4 days, showing the lack of spread of RABV to passing fibers or local neurons: no labeling is found in the VII nucleus, adjoining the nucleus reticularis magnocellularis (RMc, 2°), although ascending VII axons cross the heavily infected RPc (2°). RABV immunoperoxidase detection was based on use of a primary antibody that was not very sensitive, and produced a high level of background staining (the tissue is not counterstained). Bars: A,B,C: 150 µm; D,F,G: 400 µm; E: 100 µm; H: 150 µm.

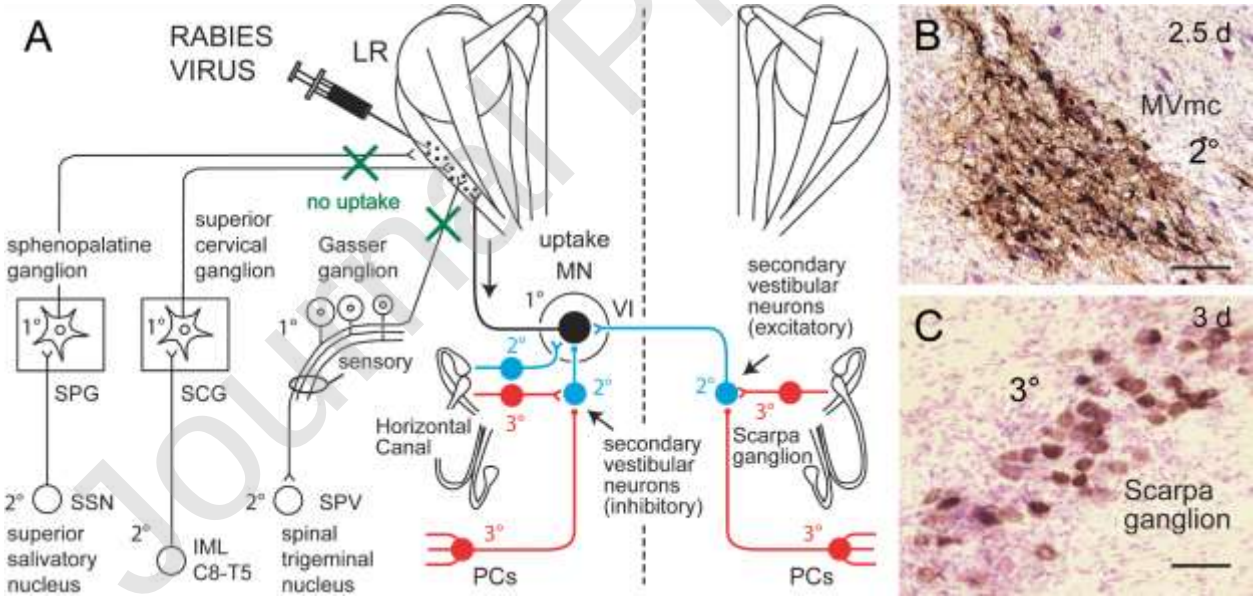

Fig. 5. Pathways of propagation of rabies virus (RABV) strain CVS-11 (FR) after inoculation into the left lateral rectus (LR) muscle in macaque monkeys (Ugolini et al., 2006). **(A)** is modified

with permission from "Ugolini, G. 2008. Use of rabies virus as a transneuronal tracer of neuronal connections: implications for the understanding of rabies pathogenesis. Dev. Biol. (Basel), 131, 493-506". Uptake and transneuronal propagation of rabies virus occurs exclusively via the motor route (first-order neurons, 1°: LR motoneurons, MN in the abducens, VI, nucleus), with no propagation in sensory, sympathetic or parasympathetic pathways that innervate the same muscle. [Sensory pathways: first-order neurons (1°), Gasser ganglion; second-order neurons (2°), spinal trigeminal nucleus. Sympathetic pathways: first-order neurons (1°), superior cervical ganglion, SCG; second-order neurons (2°), intermediolateral cell group, IML, of spinal segments C8-T5. Parasympathetic pathways: first-order neurons (1°), sphenopalatine ganglion, SPG; second-order neurons (2°), superior salivatory nucleus, SSN]. Retrograde transneuronal transfer from MN (first-order, 1°, black) involves sequentially second-order neurons (2°, blue) at 2.5 days and third-order (3°, red) at 3 days, as exemplified here by a schematic representation of the horizontal vestibulo-ocular reflex (VOR) circuitry to singly innervated (SIF, 'fast') LR MN. Retrograde transneuronal transfer of rabies virus involves all known connections, including both excitatory neurons (forked synapses) and inhibitory neurons (bouton synapses). In this model, labeling of the vestibular (Scarpa's) ganglia in the inner ear occurs ipsilaterally at 2.5 days (second-order neurons of linear VOR pathways) and bilaterally at three days (third-order neurons of VOR pathways) (see C). **(B)** Rabies immunolabeled second-order neurons (2°) in the contralateral medial vestibular, magnocellular (MVmc, excitatory neurons of VOR pathways), labeled at 2.5 days. **(C)** Third-order neurons (3°) in Scarpa's ganglion, labeled at 3 days (see A). The infection of Scarpa's ganglion is a striking example of centrifugal spread of rabies virus to sensory ganglia that is mediated by retrograde transneuronal transfer occurring during the asymptomatic period. Scale bars: 200 µm in B, 100 µm in C.

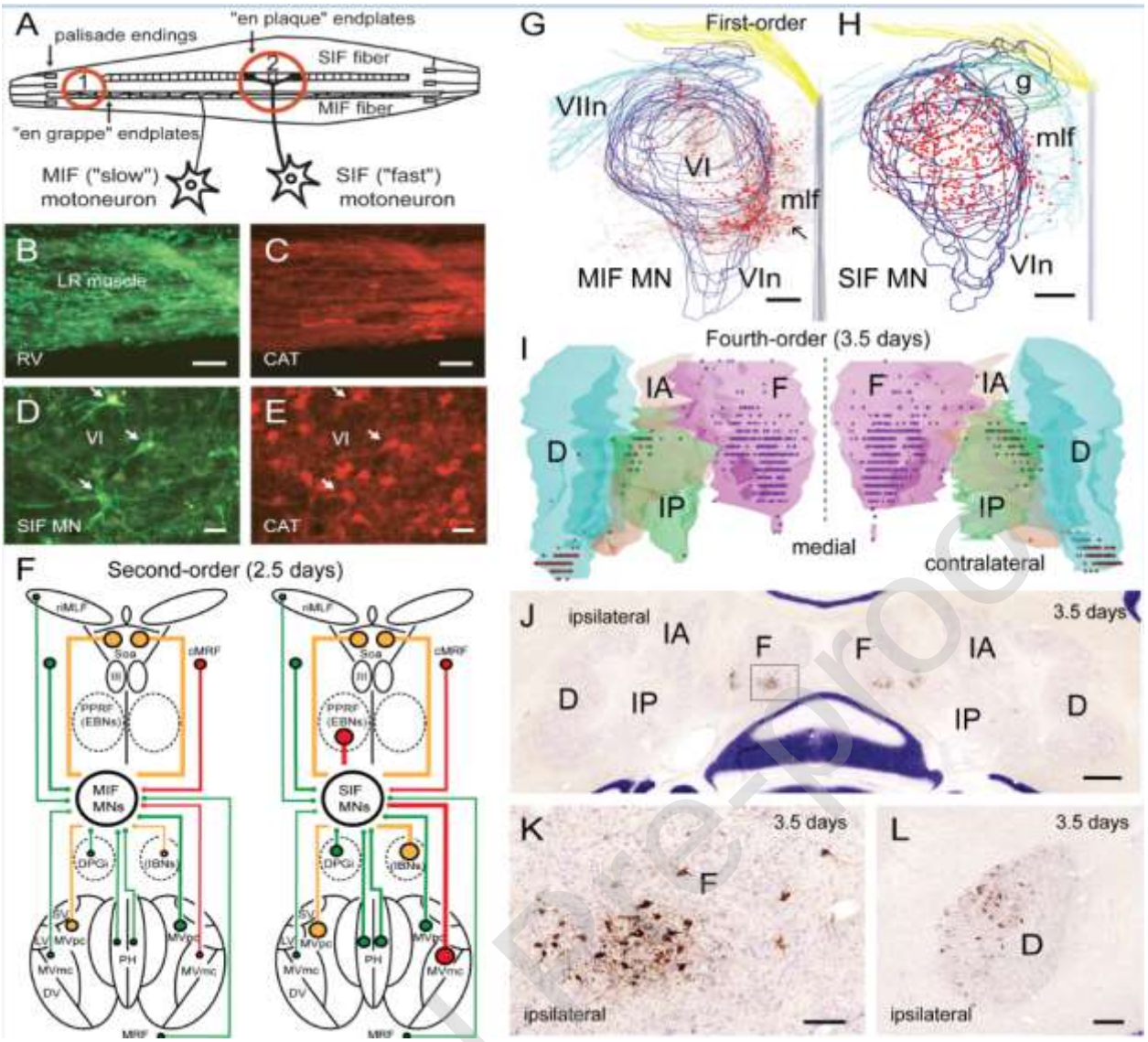

Fig. 6. Retrograde transneuronal transfer of rabies virus (RABV) strain CVS-11 (FR) from the left lateral rectus (LR) muscle in primates: exclusive uptake from abducens (VI) motoneurons, MN (first-order) and retrograde transneuronal transfer (to second order premotor populations at 2.5 days, third-order at 3 days and forth-order at 3.5 days). Modified with permission from "Ugolini G., Klam, F., Doldan Dans, M., Dubayle, D., Brandi, A.M., Büttner-Ennever, J., Graf, W., 2006. Horizontal eye movement networks in primates as revealed by retrograde transneuronal transfer of rabies virus: differences in monosynaptic input to 'slow' and 'fast' abducens motoneurons. J. Comp. Neurol. 498, 762-785" and "Prevosto, V., Graf, W., Ugolini, G., 2017. The control of eye movements by the cerebellar nuclei: polysynaptic

projections from the fastigial, interpositus posterior and dentate nuclei to lateral rectus motoneurons in primates. Eur. J. Neurosci. 45, 1538-1552". **(A)** Differences in uptake by multi-innervated (MIF, 'slow') and singly innervated (SIF, 'fast') MN after injection of RABV into the distal (1) and central (2) part of the muscle. Distal injections (1) involve selectively 'en grappe' endplates of MIF MN. Only central muscle belly injections (2) involve 'en plaque' motor endplates of SIF MN (see topographical differences of infected MIF and SIF MN in G, H). **(B-E)** Dual color immunofluorescence for RABV (FITC, green) and choline acetyltransferase (CAT) as MN marker (Cy3, red) in the LR muscle (B,C) and in the abducens (VI) nucleus (D,E). (B) LR muscle: the injection area can be identified because of viral uptake. (C) Motor endplates (CAT-positive) in the same section. (D,E) Dual immunolabeling of SIF MN (injection 2 in A): infected MN (D) express CAT at normal levels (E, arrows). **(F)** Differences in the second-order populations providing monosynaptic input to MIF (left) and SIF MN (right) labeled at 2.5 days after distal or central LR muscle injection (A). Modified from Prevosto et al., 2017. Note synchronous labeling of major and minor second-order projections (marker size and line thickness: projection strength). Only second-order populations known to receive projections from the cerebellar nuclei are included here (see Ugolini et al., 2006 for all pathways). [Red neuronal markers and forked synapses: excitatory neurons; yellow neuronal markers and bouton synapses: inhibitory; green neuronal markers and empty bouton synapses: noncharacterized or mixed populations. MIF MN (left): strong inputs from supraoculomotor area (SOA) (vergence), central mesencephalic reticular formation (cMRF), parvocellular medial vestibular nucleus (MVpc); other inputs from prepositus hypoglossi (PH), caudal medullary medial reticular formation (MRF) (gaze holding, fixation and smooth pursuit), rostral interstitial nucleus of the medial longitudinal fasciculus, riMLF (vertical bursters), dorsal paragigantocellular reticular formation (DPGi), magnocellular medial vestibular nucleus (MVmc). SIF MN (right): in addition to cell groups also targeting MIF MN, SIF MN receive inputs from saccade bursters [excitatory burst neurons (EBNs), in ipsilateral

paramedian pontine reticular formation (PPRF), inhibitory burst neurons (IBNs), in contralateral DPGi] and angular vestibulo-ocular reflex pathways (excitatory: contralateral MVmc, inhibitory: ipsilateral MVpc). Other abbreviations: DV, descending vestibular nucleus; LV, lateral vestibular nucleus; SV, superior vestibular nucleus; III, oculomotor nucleus.] **(G, H)** Three-dimensional (3D) reconstructions of the VI nucleus (dark blue outlines) (first-order): note major differences in topography of MIF MN (G) (injection 1 in A) and SIF MN (H) (injection 2 in A). Large red dots: MN cell bodies; small dots in G: MN dendrites. Light blue outlines in G,H: descending limb of the facial nerve (VIIn). Green outlines in H: genu (g) and ascending limb of VIIn. Gray vertical lines: midline; mlf, medial longitudinal fasciculus. Yellow: brainstem dorsal surface. **(I–L)** Cerebellar nuclei: 3D reconstructions (200 µm spacing among sections) (I) and cross sections (J-L) at 3.5 days, showing the topography of fourth-order neurons which influence SIF motoneurons trisynaptically. In (I), cerebellar nuclei and labeled neurons (dots) are color-coded (blue: dentate, D; green: interpositus posterior, IP; orange-brown: interpositus anterior, IA; magenta: fastigial, F). Note labeling in F nuclei mostly caudally (F oculomotor region), rostral ventrolateral IP (far response) and caudal D (oculomotor region). **(J-L)** Examples of RABV immunolabeled fourth-order neurons in caudal F and ventrolateral IP (J and K) and caudal D (L). RABV immunolabeling was based on a sensitive immunoperoxidase protocol and combined with cresyl violet counterstaining. Bars= B,C: 100 µm; D,E: 50 µm; G, H: 400 µm; J: 1000 µm; K: 150 µm; L: 200 µm.

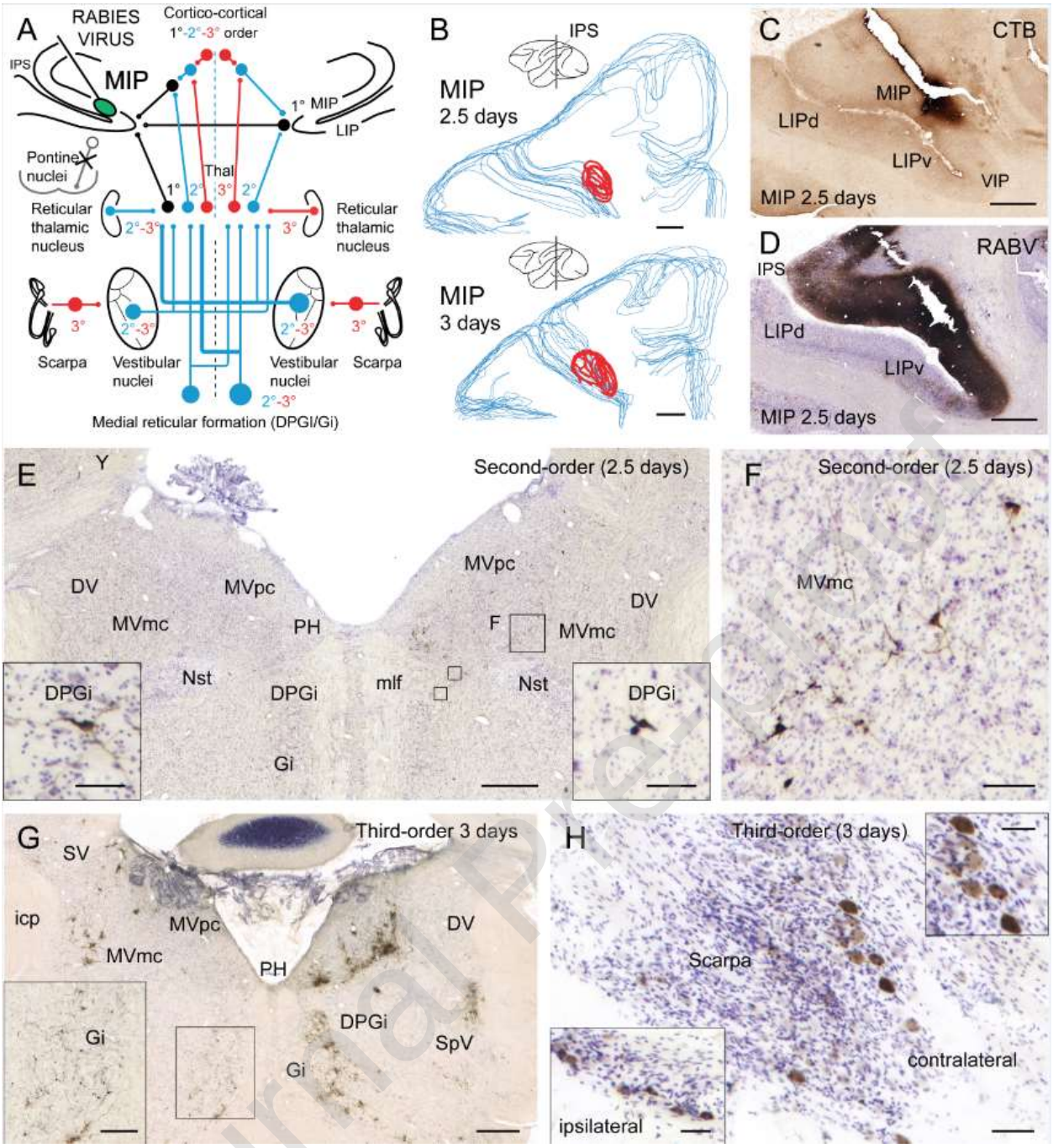

Fig. 7. Retrograde transneuronal transfer of rabies virus (RABV) strain CVS-11 (FR) to the vestibular nuclei, medial reticular formation and vestibular (Scarpa's) ganglia after injection of a mixture of RABV and Cholera toxin B, CTB into the left medial intraparietal area (MIP). Modified with permission from "Ugolini G., Prevosto V., Graf, W., 2019. Ascending vestibular pathways to parietal areas MIP and LIPv and efference copy inputs from the medial reticular

formation: functional frameworks for body representations updating and online movement guidance. Eur. J. Neurosci. 50, 2988-3013". **(A)** Summary diagram: 1° (black), first-order neurons (conventional tracer, CTB) in the ipsilateral thalamus and cortical areas (ipsilateral cortico-cortical inputs, callosal inputs from homotopic MIP portions of the right hemisphere). 2° (blue), second-order neurons labeled transneuronally (RABV) at 2.5 days in the vestibular nuclei and medullary medial reticular formation bilaterally, in the ipsilateral thalamic nuclei and reticular thalamic nucleus, and in the contralateral thalamus (the latter reflecting projections to the right MIP). For inputs from the vestibular nuclei and medial reticular formation, marker size and line thickness indicate the strength of the projections. 3° (red), third-order neurons labeled at 3 days bilaterally in Scarpa's ganglia, in the vestibular nuclei, reticular formation and in the thalamus. Anterograde transneuronal transfer of RABV (e.g., to the pontine nuclei) did not occur. IPS: Intraparietal sulcus. **(B)** Three-dimensional reconstructions of the MIP injection area (red). **(C)** and **(D)** Photomicrographs of adjoining sections at the MIP injection site, immunolabeled for CTB and RABV. The injection area is easily identifiable with CTB (C) but not with RABV (D) at 2.5 days, because of strong RABV immunolabeling of short-distance projections neurons in the IPS (second-order). Other abbreviations: LIPd: dorsal lateral intraparietal area (LIP); LIPv: ventral LIP; VIP: ventral intraparietal area. **(E)** and **(F)** Caudal medulla: examples of RABV immunolabeled second-order neurons in the medial vestibular nucleus, magnocellular (MVmc) mostly contralaterally, and medial reticular formation (dorsal paragigantocellular reticular formation, DPGi, and gigantocellular reticular formation, Gi) that target MIP disynaptically (2.5 days). Framed areas in (E) are enlarged in insets in (E) (DPGi) and (F) (MVmc). **(G, H)** RABV immunolabeled third-order neurons in vestibular nuclei and medial reticular formation (DPGi, and Gi) (G) and vestibular (Scarpa's) ganglia (H) at the trisynaptic time point (3 days). (G) Caudal medulla: bilateral labeling in the VN is still most prominent in the contralateral MVmc. At this time point, bilateral labeling in the medial reticular formation ipsilaterally (enlarged in inset) and

contralaterally includes distal cell processes extending into the medial longitudinal fasciculus (mlf). (H) Third-order neurons labeled in the contralateral and ipsilateral (inset) Scarpa's ganglia. Initial labeling of ganglion cells does not include axons. RABV immunolabeling in D-K was combined with cresyl violet counterstaining. Other abbreviations: Icp, inferior cerebellar peduncle; MVpc, medial vestibular, parvocellular; Nst, nucleus of the solitary tract; PH, prepositus hypoglossi; SpV, spinal trigeminal nucleus; Y, y group. Scale bars: 2000 µm in A-D; 1000 µm in E, G; 400 µm in inset in G; 100 µm in H; 50 µm in F and insets in E.

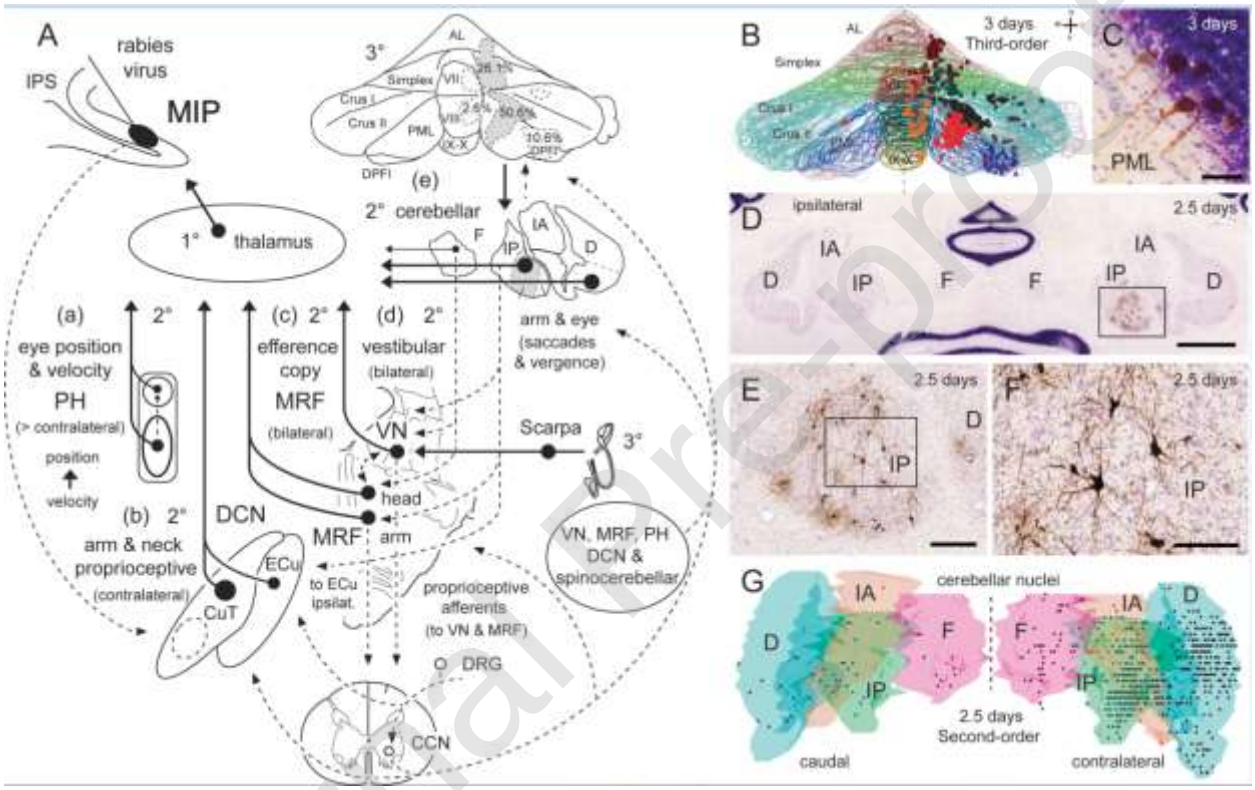

Fig. 8. (A) Simplified diagram summarizing ascending polysynaptic pathways to the rostral medial intraparietal area (MIP), revealed by retrograde transneuronal transfer of rabies virus (RABV) (CVS-11 FR). Adapted with permission from "Ugolini G., Prevosto V., Graf, W., 2019. Ascending vestibular pathways to parietal areas MIP and LIPv and efference copy inputs from the medial reticular formation: functional frameworks for body representations updating and online movement guidance. Eur. J. Neurosci. 50, 2988-3013". Labeled pathways are shown

by black markers, solid lines and large arrows (markers size indicates projection strength). For bilateral pathways only the dominant side is shown. (1°): First-order; (2°) disynaptic pathways; (3°) trisynaptic. Inputs to rostral MIP: (a) eye velocity and position signals (prepositus hypoglossi, PH, vertical arrow: caudo-rostral velocity-to-position transformation; Prevosto et al., 2009); (b) arm and neck proprioceptive inputs from the dorsal column nuclei, DCN (2°) (cuneate pars triangularis, CuT, and external cuneate, ECu, Prevosto et al., 2011); (c) efference copy pathways from arm- and head movement-related reticulospinal domains (medial reticular formation, MRF) (2°); (d) vestibular inputs from the vestibular nuclei (VN) (2°) and Scarpa's ganglia (3°) (Ugolini et al., 2019, see also Fig. 7); (e) major cerebellar output channels from dentate (D) and interpositus posterior (IP, arm- and eye movements-related domains, in dark and light grey respectively) (2°) and related cerebellar cortical modules (3°) (paramedian lobule, PML/Crus II 50.6%, Simplex/Anterior lobe, AL 26.1%; dorsal paraflocculus, DPFl 10.6%); note only minor inputs from rostral fastigial (F) and cerebellar vermis, 2.6% (Prevosto et al., 2010) (see B-G). Rostral MIP and the labeled PH, DCN, VN, MRF and cerebellar domains form a tightly interconnected circuit for multisensory guidance and online control of arm movements, eye-hand coordination coupling and internal models implying the posterior parietal cortex and cerebellum. Known main interconnections and pathways (unlabeled) are indicated by open markers, stippled lines and small arrows: proprioceptive afferents to DCN, VN, MRF and cerebellum; inputs to the labeled cerebellar domains from PH, DCN, VN, MRF; (crossed) cerebellar output pathways to VN, MRF and DCN (ECu); VN-MRF interconnections; vestibulo- and reticulospinal pathways; MIP projections to DCN (see Prevosto et al., 2009, 2010, 2011; Ugolini et al., 2019). Other abbreviations: CCN, central cervical nucleus; DRG, dorsal root ganglia; IA, Interpositus anterior; IPS, intraparietal sulcus. **(B-G)** Cerebellar output channels to MIP. Modified with permission from "Prevosto, V., Graf, W., Ugolini, G., 2017. Cerebellar inputs to intraparietal cortex areas LIP and MIP: functional frameworks for adaptive control of eye movements, reaching and arm/eye/head

movement coordination. Cereb. Cortex 20, 214-228". (B) Three-dimensional (3D) reconstructions of the cerebellar cortex: Purkinje cell (PCs) providing trisynaptic inputs to MIP (3 days). 3D reconstructions were made using Neurolucida (200 µm spacing). Cerebellar divisions and PCs are color coded. (C) RABV immunolabeled PCs in PML. (D-G): Cerebellar nuclei (disynaptic inputs, at 2.5 days) (D-F) RABV immunolabeled neurons in ventrolateral IP and D; boxed area in (D) is enlarged in (E) (ventrolateral IP); high-power view in (F). (G) 3D reconstructions of the cerebellar nuclei at 2.5 days (disynaptic inputs to MIP). Cerebellar nuclei and labeled neurons (dots) are color-coded as in Fig. 6. Bars: 50 µm in C; 2000 µm in D; 400 µm in E; 200 µm in F. Polysynaptic inputs relayed to a given cortical area via the thalamus can be reliably identified by retrograde transneuronal transfer of RABV (as shown here), but not with single-step tracers or monosynaptically restricted viral tracers, because of the convergence of multiple input pathways to the same thalamic nuclei, and major overlap of thalamocortical populations supplying different cortical areas.

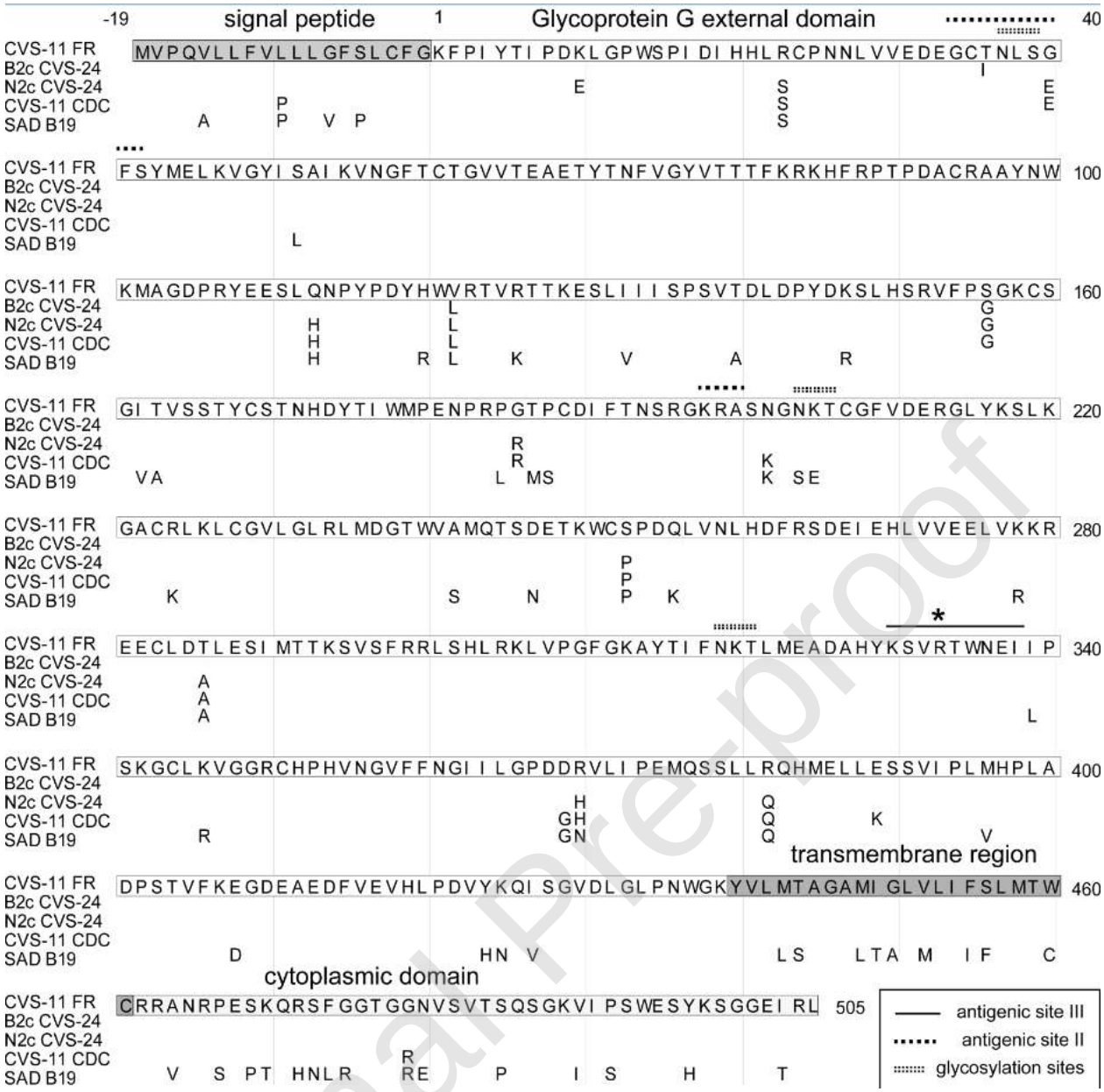

Fig. 9. Rabies virus (RABV) glycoprotein G: Comparison of the amino acid (AA) sequence of the 'french' CVS-11 (FR), used for transneuronal tracing in European laboratories) (accession n° 1106215A, Seif et al., 1985), the B2c and N2c variants of CVS-24 (n° AAB97691 and n° AAB97690, Morimoto et al., 1998) and CVS-11 from the Atlanta Center for Disease Control (CDC) (n° AAC34683, Smith et al., 1973). The attenuated SAD B19 strain (accession n° M31046.1, Conzelmann et al., 1990) is included for comparison. The figure shows the full AA sequence of CVS-11 (FR) (top), and AA differences in the other RABV strains. Different

shading (top line) is used to distinguish the signal peptide, the G external domain, transmembrane region and cytoplasmic domain. The main antigenic sites III (AA 330-338) and II (34-42 and 198-200), and the three putative glycosylation sites (NXT or NXS) are indicated. AA position is numbered (AA residues are as follows: A, Ala; C, Cys; D, Asp; E, Glu; F, Phe; G, Gly; H, His; I, Ile; K, Lys; L, Leu; M, Met; N, Asn; P, Pro; Q, Gln; R, Arg; S, Ser; T, Thr; V, Val; W, Trp; Y, Tyr). In all strains, AA 333 (asterisk) is R (Arg), associated with virulence (see # 5.4). The G of CVS-11 (FR) is very similar to CVS-24 B2c (3 AA difference), and diverges from CVS-24 N2c (11 AA) and CVS-11 from CDC (15 AA). The B2c and N2C variants differ in 10 AA. N2c CVS-24 and CVS-11 CDC differ in 4 AA. The G of SAD B19 highly diverges from all CVS strains.

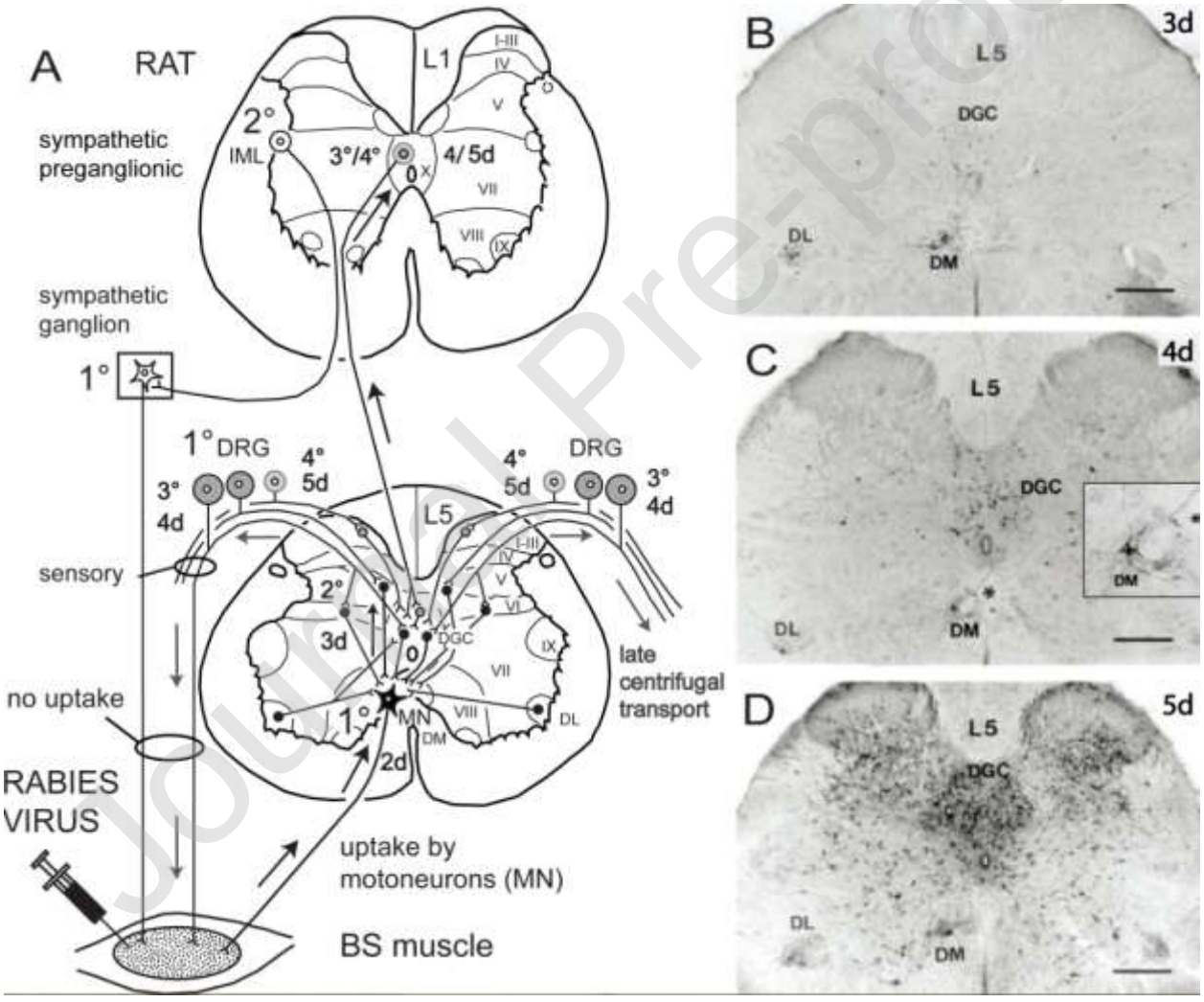

Fig. 10. (A) Kinetics of propagation of rabies virus (RABV) (CVS-11 strain) to the spinal cord after inoculation into the left bulbospongiosus (BS) muscle in rats. **(B–D)** RABV-immunolabeled neurons in the L5 spinal segment at 3, 4, and 5 days (d). Left: ipsilateral. Modified with permission from "Tang, Y., Rampin, O., Giuliano, F., Ugolini, G., 1999. Spinal and brain circuits to motoneurons of the bulbospongiosus muscle: retrograde transneuronal tracing with rabies virus. J. Comp. Neurol. 414, 167-192" and "Ugolini, G. 2008. Use of rabies virus as a transneuronal tracer of neuronal connections: implications for the understanding of rabies pathogenesis. Dev. Biol. (Basel), 131, 493-506". **(A)** Uptake and transneuronal transfer of RABV occurs exclusively from BS motoneurons (MNs) (first-order, 1°) in the ipsilateral dorsomedian (DM) nucleus) (at 2 days), with no uptake by sensory neurons (in the ipsilateral dorsal root ganglia, DRG, at L5-S1), or sympathetic neurons (1°: sympathetic ganglia; second-order, 2°: pregaglionic neurons in the intermediolateral cell group, IML, of upper lumbar and lower thoracic segments). Infected BS MN remain viable and do not increase in numbers with time **(B–D)** although they are linked by gap junctions, showing that RABV does not propagate through gap junctions. From BS MNs, RABV propagates by retrograde transneuronal transfer at chemical synapses to 2° order neurons (see **(A)**, 2°, black) at 3 days, and higher-order neurons (3°, dark gray; 4°, light gray) at 4 and 5 days p.i. The sympathetic populations supplying the BS muscle remain uninfected. DRG infection occurs bilaterally only at 4 and 5 days and is mediated by retrograde transneuronal transfer to DRG through their spinal connections **(A)**, showing that centrifugal migration of RABV can already occur during the asymptomatic period. From infected DRG, late onset centrifugal transport to end-organs may occur later, via their sensory innervation. Other abbreviations: dorsal gray commissure, DGC; dorsolateral nucleus, DL; I–X: spinal laminae. Scale bars: 900 mm.